

Supramolecular assemblies based on crown- and phosphoryl-substituted phthalocyanines and their metal complexes in microheterogeneous media*

N. F. Goldshleger,^{a*} M. A. Lapshina,^a V. E. Baulin,^b A. A. Shiryaev,^c Yu. G. Gorbunova,^{c,d} and A. Yu. Tsivadze^{c,d}

^aInstitute of Problems of Chemical Physics, Russian Academy of Sciences,
1 prosp. Akad. Semenova, 142432 Chernogolovka, Moscow Region, Russian Federation.
E-mail: nfgold@icp.ac.ru

^bInstitute of Physiologically Active Compounds, Russian Academy of Sciences,
1 Severnyj proezd, 142432 Chernogolovka, Moscow Region, Russian Federation.
E-mail: mager1988@gmail.com

^cA. N. Frumkin Institute of Physical Chemistry and Electrochemistry, Russian Academy of Sciences,
Build. 4, 31 Leninsky prosp., 119071 Moscow, Russian Federation.

^dN. S. Kurnakov Institute of General and Inorganic Chemistry, Russian Academy of Sciences,
31 Leninsky prosp., 119991 Moscow, Russian Federation.

The review is concerned with studies on peculiar features of supramolecular organization of phthalocyanines (Pc) bearing complex-forming substituents (15-crown-5, 2-oxyphenylphosphonic acid residues) in organized aqueous microheterogeneous media based on cationic and anionic surfactants, bile salts (BS) including sodium deoxycholate (SDC), as well as polyelectrolytes and amphiphilic polymers including a phosphate buffer (pH 7.4). Organized, SDC-based fluorescence-active phthalocyanine-containing hydrogels obtained for the first time are also considered. *In vitro* accumulation and localization of Pc in human cervical adenocarcinoma cells, HeLa, as well as the photochemical and sensitizing properties of Pc including light cytotoxicity and photoinduced generation of reactive oxygen species were demonstrated taking octa-crown-substituted magnesium phthalocyaninate as an example.

Key words: supramolecular assembly, phthalocyanines, solubilization, crown ethers, 2-oxyphenylphosphonic acid, bile salts, surfactants, photosensitizer.

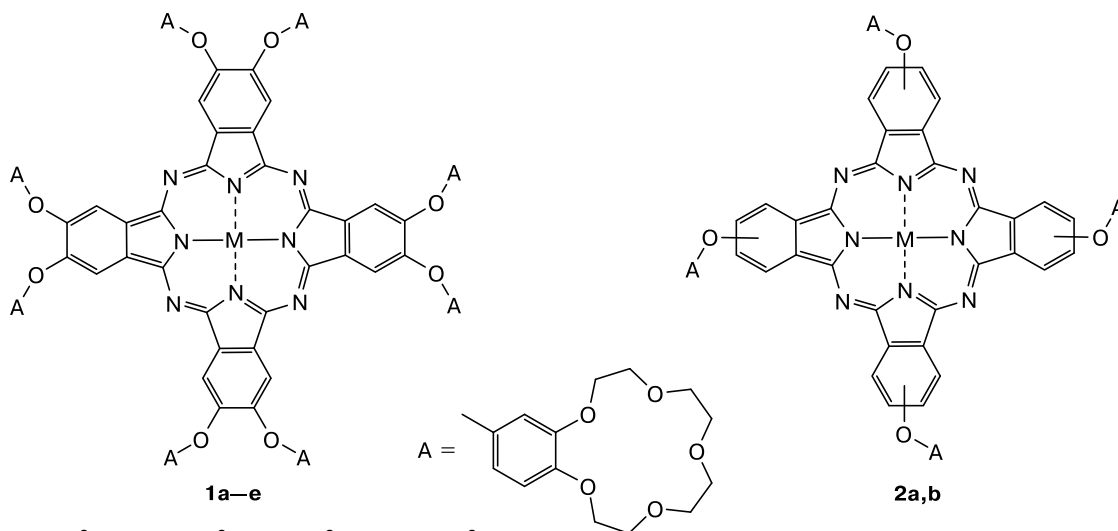
Introduction

Supramolecular chemistry is a field of knowledge which studies self-organization processes involving molecules that are often structurally or functionally similar to biological molecules and resulting in the formation of supramolecular assemblies and other objects that held together through intermolecular interactions (hydrogen bonds, ion-ion, ion-dipole, van der Waals, π – π -stacking, CH– π , hydrophobic, coordination interactions, *etc.*). The term "supramolecular chemistry" and the basic concepts were introduced by J.-M. Lehn in 1978.¹ The energy of intermolecular interactions is much lower than that of covalent bonds in organic molecules and rarely reaches values of the order of 100 kJ mol^{–1}. For instance, the energy of CH– π -interactions falls in the range of 0.84–10.5 kJ mol^{–1}.² Numerous weak noncovalent interactions stabilize supramolecular assemblies, being responsible for reversible

character of molecular association (or self-organization) reactions and for the possibility to maintain equilibria by varying external conditions. In particular, the role of supramolecular interactions in the redox reactions of the electroactive component (transition-metal complexes, metallophthalocyanine, fullerene and its derivatives) in artificial lipid matrix in aqueous medium was studied (see Refs 3 and 4 and references cited therein).

The complex-forming, electrophysical, and optical properties of phthalocyanines (Pc), metallophthalocyanines, and their supramolecular aggregates underlie a wide range of applications including catalysis, medicine, molecular electronics, and synthesis of chemosensors.^{5–7} Chemical stability, low toxicity, the absorption spectrum with a maximum in the range of 650–750 nm, and generation of reactive oxygen species (ROS) upon excitation allows one to consider Pc as potential photosensitizers for photodynamic diagnostics and photodynamic therapy (PDT) of various diseases including cancer.^{8,9} The photochemical properties of phthalocyaninates of diamagnetic main-group metals (*e.g.*, Al, Ga, Zn), namely, photostability, triplet state lifetime (it is long enough for the

* Based on the materials of the XXI Mendeleev Congress on General and Applied Chemistry (September 9–13, 2019, St. Petersburg, Russia).



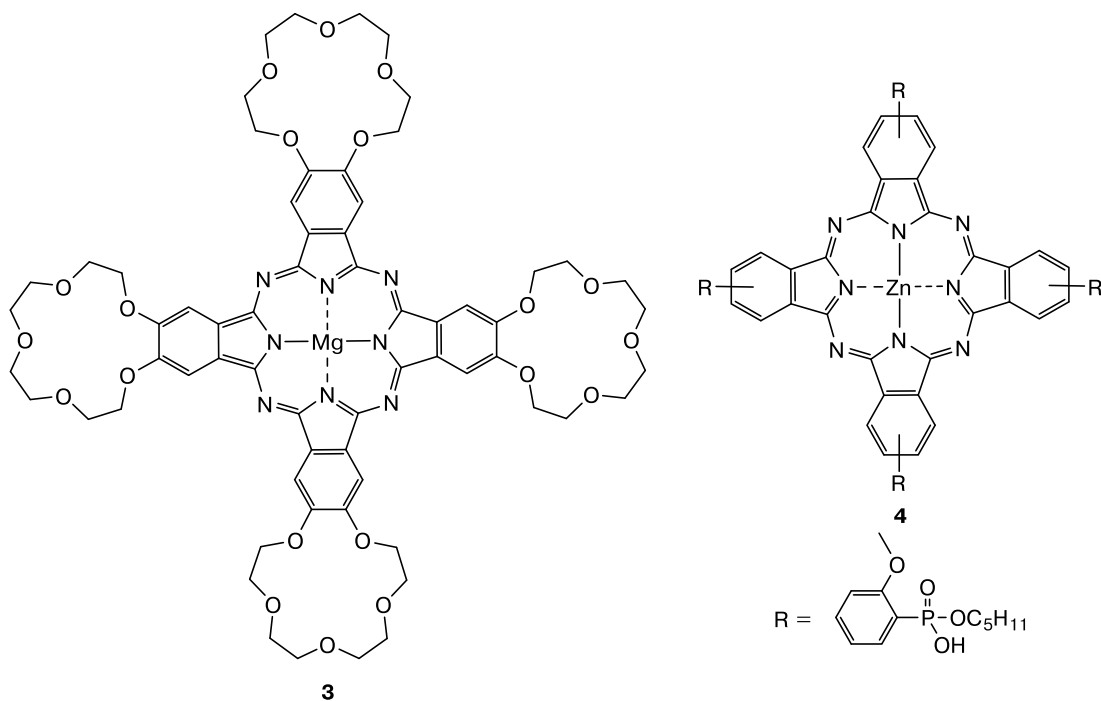
M = 2H⁺ (**1a**), Co²⁺ (**1b**, **2a**), Ni²⁺ (**1c**), Mg²⁺ (**1d**, **2b**), Zn²⁺ (**1e**)

photodynamic effect to occur), and the quantum yield of ¹O₂ to a sufficient degree of reliability meet the PDT requirements.¹⁰ Photoinduced generation of ROS (mainly singlet oxygen ¹O₂) requires that Pc be in the monomeric state in physiological conditions. The tendency to aggregation of phthalocyanines in organic and polar media becomes less pronounced upon introducing bulky substituents (alkyl, alkylaromatic, and polar groups) into the macrocycle since they produce steric hindrances to stacking (π – π)-interactions between macrocycles.

The presence of benzo-15-crown-5 moieties (either annelated^{11,12} or introduced *via* an oxygen bridge¹³) in Pc molecules enhances the solubility and favors self-organization of phthalocyanines involving a guest cation. Specific features of such a process are determined by the size and

shape correspondence between the crown ether cavity and the alkali metal ion¹⁴ and by the degree of satisfaction of the principle of multiple interactions (an increase in the number of reacting groups). The results of studies on the supramolecular organization of phthalo- and metallophthalocyanines with annelated crown ether moieties in organic solvents have been thoroughly reviewed.^{6,11,12}

In this review we summarized the results of research into supramolecular organization of poorly studied phthalo- and metallophthalocyanines containing eight or four peripheral complex-forming benzo-15-crown-5 substituents introduced *via* an oxygen bridge (compounds **1** and **2**, respectively), magnesium tetra(15-crown-5)phthalocyaninate **3**, and phosphoryl-containing zinc phthalocyaninate bearing four 2-oxyphenylphosphonic acid resi-



dues **4** in phosphate buffer (pH 7.4) and in aqueous organized microheterogeneous media.

We used cationic surfactants including cetyltrimethylammonium bromide (CTAB) and cetyltriphenylphosphonium bromide (CTPB), anionic surfactants including sodium dodecylsulfate (SDS) and sodium dodecylbenzenesulfonate (SDBS), as well as bile salts (BS) and solutions of polyelectrolytes and amphiphilic polymers. Combining the broad range of surfactants with different properties (charge, critical micelle concentrations (cmc), micelle shape, ability to create a biologically similar environment) and various methods of investigation, such as electronic spectroscopy, fluorescence spectroscopy, small-angle X-ray scattering (SAXS), and fluorescence microscopy made it possible to determine conditions for the existence of Pc in the monomeric state in aqueous media in the presence of traditional and biocompatible surfactants. The structural formulas of the surfactants discussed in the review are shown in Fig. 1.

The review presents the results of studies of supramolecular, sodium deoxycholate (SDC) based fluorescence-active hydrogels containing magnesium octa[(4'-benzo-15-crown-5)oxy]phthalocyaninate **1d** and zinc octa[(4'-benzo-15-crown-5)oxy]phthalocyaninate **1e**, obtained for the first time. The compounds were examined as potential photosensitizers and specific features of their

in vitro accumulation and localization in human cervical adenocarcinoma cells, HeLa, as well as the photochemical and sensitizing properties including light cytotoxicity and photoinduced generation of ROS were established. The results obtained are given below.

Crown-ether-substituted phthalocyanines in organic and polar media

A series of our publications on solubilization of crown-substituted Pc and their supramolecular organization in aqueous media began with the study of the state of octa[(4'-benzo-15-crown-5)oxy]phthalocyanine **1a** and its complexes with Co^{2+} and Ni^{2+} (**1b** and **1c**, respectively) in organic solvents, mixed systems, and polar (including aqueous) media, in the presence of salts containing different cations.¹⁵ The solvents used were CH_2Cl_2 having low polarity and two polar solvents, propylene carbonate characterized by a donor number (DN) of 15.1 and water (DN = 33.2)¹⁶. The solubility of H_2O in 100 g of solvent was 0.198 g for dichloromethane and 21.2 g for propylene carbonate. The absorption spectra of compound **1b** and other related Pc in CH_2Cl_2 solution appeared to be typical of monomers; no deviation from the Bouguer—Lambert—Beer law was observed in the concentration range of $2.5 \cdot 10^{-6}$ — $2.5 \cdot 10^{-5}$ mol L^{-1} . The half-width of

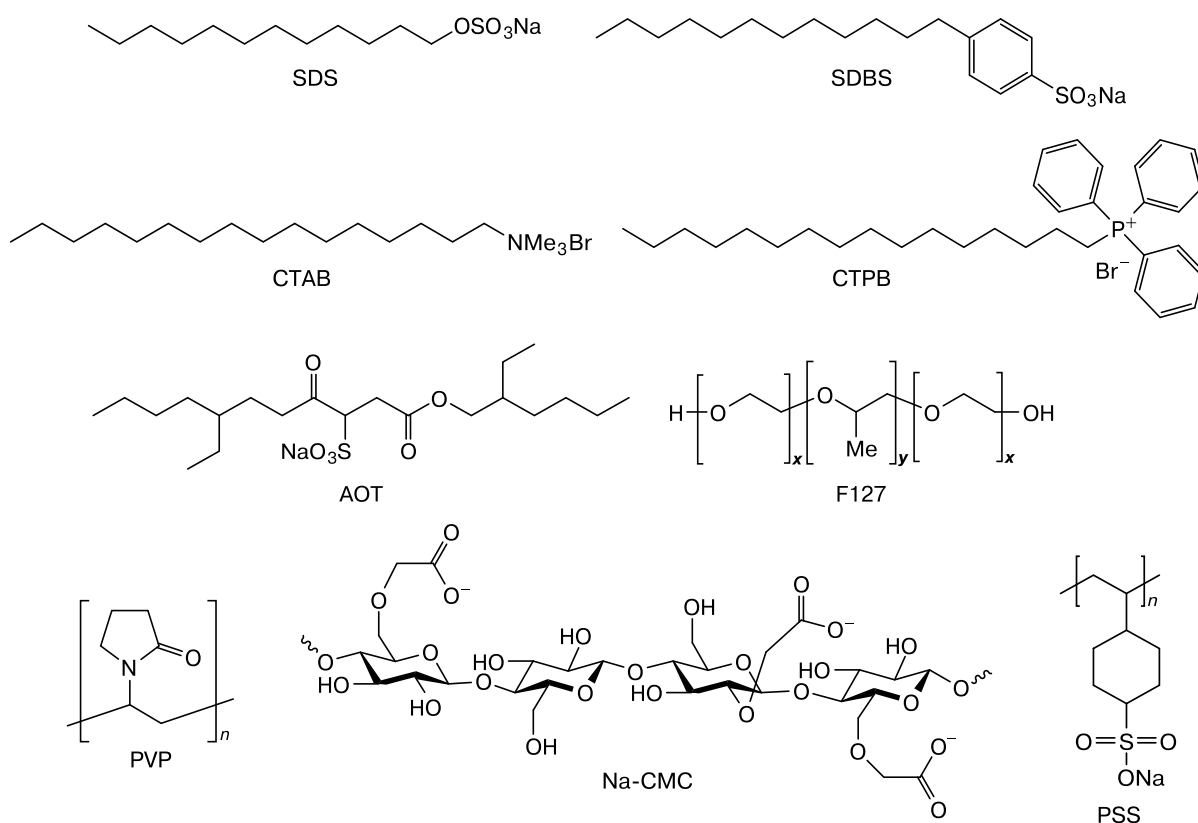


Fig. 1. Surfactants, polyelectrolytes and amphiphilic polymers discussed in the review.

the Q-band (at $\lambda_{\max} = 673$ nm; extinction coefficient $\varepsilon = 1.47 \cdot 10^5$ L mol⁻¹ cm⁻¹) is ~ 500 cm⁻¹. From the electronic absorption spectrum (EAS) of compound **1b** at C₂H₅OH/CH₂Cl₂ = 3 it follows that Pc molecules form associates even at low concentrations. As the medium polarity increases, the optical density decreases in the region of the long-wavelength maximum of the Q-band and increases in region of the H-dimer at 630 nm.¹⁵ The presence of tetraoctylammonium bromide or Bu₄NBF₄ in solutions of compounds **2a** or **1b** in dichloromethane has almost no effect on the position of the Q-band maximum (Fig. 2, spectra 1 and 2) in contrast to the films of the same compounds prepared by the drop method on quartz (Fig. 2, spectra 3 and 4). Spectrum 4 of cobalt tetra[4'-benzo-15-crown-5)oxy]phthalocyaninate **2a** recorded in the absence of Bu₄NBF₄ exhibits a bathochromic shift of the Q-band maximum and corresponds to the monomeric state of the compound, whereas spectrum 3 recorded in the presence of salt in the condensed phase is indicative of mainly aggregated state of the metallophthalocyanine.

Structurally organized composites. Aggregation of Pc containing crown ether substituents at the periphery of the macrocycle is influenced by both the solvent and the chemical composition of salts used. In particular, the EAS of compound **1c** in propylene carbonate corresponds to a rather stable suspension when recorded in the absence of (tBu₄N)BF₄ and to H-dimer characterized by a Q-band at 630 nm when recorded in the presence of a salt. Taking into account the size of cations and crown ether cavities (Table 1), the EAS of metallophthalocyanine **1c** in propylene carbonate recorded in the presence of NaClO₄ and KClO₄ corresponds to a monomer and dimer, respectively.

In aqueous media, potassium cations favor dissolution of compounds **1a–c** with the formation of stable charged forms (heteronuclear complexes). For instance, structurally organized of films the composition K⁺_xM[(B15C5O)₈Pc]/

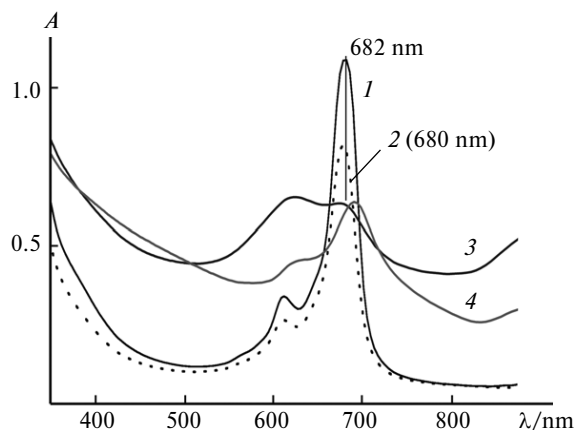


Fig. 2. Electronic absorption spectra of solution of compound **2a** in dichloromethane (1, 2) and films on quartz (3, 4) in the presence (1, 3) and in the absence (2, 4) of tetraoctylammonium bromide.

Table 1. Diameters of cations (d_1) and crown ether cavities (d_2)¹⁷

Cation	$d_1/\text{Å}$	Crown ether	$d_2/\text{Å}$
Li ⁺	1.36	12-Crown-4	1.2–1.5
Na ⁺	1.9	15-Crown-5	1.7–2.2
K ⁺	2.66	18-Crown-6	2.6–3.2
Cs ⁺	3.38	21-Crown-7	3.4–4.3
Et ₄ N ⁺	8.2		
^t Bu ₄ N ⁺	11.6		
(C ₈ H ₁₇) ₄ N ⁺	19		

PSS⁻ (PSS⁻ = [CH₂CH(C₆H₄SO₃⁻)]_n) were assembled from ultrathin layers of differently charged ions using the layer-by-layer approach¹⁸ which is used to fabricate advanced functional materials. Dissolution of Pc in polar (including aqueous) media is favored by the large number of substituents and by the presence of the oxygen bridge responsible for the mobility of the crown ether fragments and for the possibility to obtain identical stacking phthalocyanine structures containing K⁺ or ^tBu₄N⁺ cations.¹⁵ Methods for the synthesis of certain new functionalized phthalocyanines as well as Mg^{II}, Co^{II}, Cu^{II}, Zn^{II}, and Ni^{II} phthalocyaninates bearing peripheral benzo-15-crown-5-, phosphoryl- and pyridine-containing substituents have been reviewed.¹⁹ The results of studies on the aggregation state of these compounds in water and in aqueous salt solutions were generalized and the possibility of electrostatic immobilization of the compounds in question in the form of self-assembled systems composed of ultrathin ionic layers on quartz and conductive glasses was considered.

Crown-substituted phthalocyanines in microheterogeneous surfactant-based systems as media. Conditions for preventing aggregation of crown-substituted Pc in aqueous media and for creating a biocompatible environment were established using surfactants, whose structural differences specify the character of packing and the shape of micellar aggregate,²⁰ and the possibility to form guest–host complexes.

Molecules of traditional surfactants, e.g., SDS, SDBS, and CTAB have well-defined hydrophilic and lipophilic groups, namely, a relatively small polar group ("head") and a long flexible (alkyl or alkylaromatic) radical. This structure provides the possibility to form spherical surfactant micelles with high hydrophilic-lipophilic balance (HLB) in aqueous medium.²⁰ For instance, SDS is the most hydrophilic surfactant (HLB = 40 on Griffin's scale). On this scale, HLB = 10 is an approximate boundary between lipophilic and hydrophilic surfactants. The properties of selected surfactants are listed in Table 2.

The behavior of aqueous solutions of compounds **1a,b** and **2a** in the presence of KCl and cationic and anionic surfactants including CTAB, carboxymethylcellulose sodium salt (Na-CMC, [C₆H₇O₂(OH)_{3-x}(OCH₂-

Table 2. Properties of aqueous solutions of surfactants at 25 °C

Surfactant	cmc ₁	cmc ₂	<i>N</i> _{agg}	<i>D</i> _h /nm
	mmol L ⁻¹			
SDBS	1.88 ²¹ ; 1.2 ²²	6.90; 7.72	51 ²³ ; 60 ²⁰	4.0 ²⁰
SDS	7.75 ²⁴ ; 8.9	40.4; 43.7	72 ²⁰	3.88 ²⁰
CTAB	1.6 ²⁰		61	~6
AOT	2.72 ²⁰		15 ²⁵	
SDC	2.4 ²⁶	6.5	2–5	~1.4

Note. cmc₁ and cmc₂ are the first and second critical micelle concentrations, respectively; *N*_{agg} is the aggregation number (number of surfactant molecules in a micelle), and *D*_h is the hydrodynamic diameter of micelle.

COONa)_x]_n), and SDS was studied by electronic spectroscopy.²⁷

Crown ethers can form water-soluble complexes with alkali metal cations, in particular, K⁺ ion (*d*₁ = 2.66 Å). In aqueous KCl solution, the rate and degree of dissolution of octa-crown-substituted Pc **1b** is influenced by the salt concentration. The EAS of aqueous solution of the system **1b**–KCl over crystals of compound **1b** (Fig. 3, *a*, curve 1) is characteristic of low salt concentration ($\leq 5.5 \cdot 10^{-3}$ mol L⁻¹). Absorption in the region 630 nm, a shoulder near 750 nm, and broadening of the spectral band in the shorter-wavelength region suggest the formation of aggregates of different composition. The observed bathochromic shift of the Q-band maximum to $\lambda = 750$ nm relative to the Q-band maximum in the EAS of monomer **1b** in CH₂Cl₂ is 0.189 eV, being an indirect proof of the presence of Pc nanoparticles in the solution. For instance, the Q-band maximum in the spectra of different forms of 1,4,8,11,15,18,22,25-octabutoxy-29*H*,31*H*-phthalocyanine is observed at 760 nm for acetone solution and at 872 nm for aqueous solution; the spectrum of the nanocrystalline form of this compound in water exhibits a bathochromic shift of the Q-band maximum (0.21 eV).²⁸

An increase in the KCl concentration to more than $5.5 \cdot 10^{-2}$ mol L⁻¹ causes rapid dissolution of compound **1b** and formation of a stable homogeneous solution whose optical density shows no changes with time. A maximum at 628 nm in the EAS is indicative of mainly cation-induced cofacial aggregation of macrocycles (see Fig. 3, *b*).^{15,27,29} Note that the presence of metal atom in the phthalocyanine macrocycle has no effect on the solubilization process since compound **1a** is also soluble in identical conditions.

Hydrophilic-hydrophobic Na-CMC, a general-purpose water-soluble biopolymer, exhibits suspending, stabilizing, and film-forming properties and is of interest for phthalocyanine solubilization studies. From the EAS of metallophthalocyanine **1b** in 0.64% aqueous Na-CMC solution ($\sim 5 \cdot 10^{-2}$ mol L⁻¹ per formula unit at *x* = 1) exists in aggregated state. Phthalocyanine **1a** behaves analo-

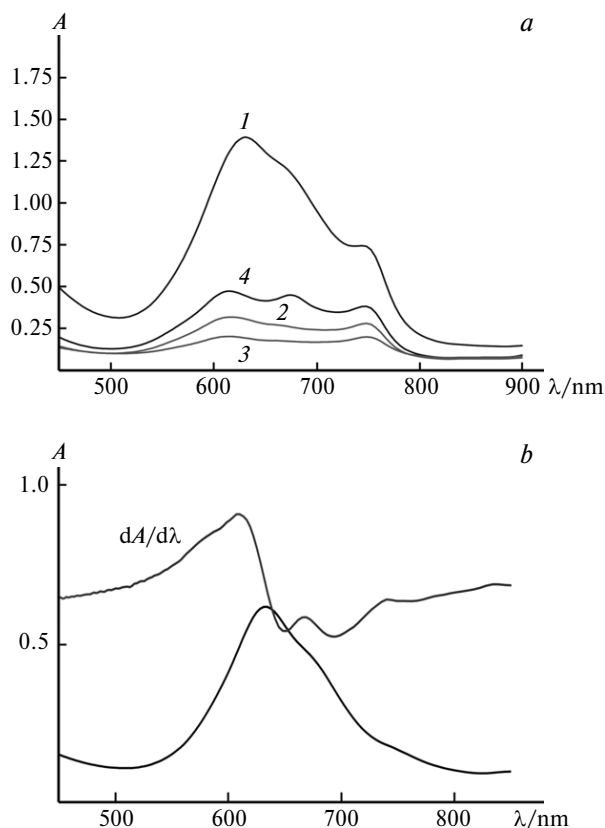


Fig. 3. Absorption spectra of aqueous solutions of compound **1b** (*a*) upon adding KCl ($[KCl] \approx 5.5 \cdot 10^{-3}$ mol L⁻¹) over crystalline **1b** (1), upon dilution with H₂O and centrifugation (2), in the presence of CTAB ($[CTAB] \sim 8.6 \cdot 10^{-3}$ mol L⁻¹) before and after centrifugation (curves 3 and 4, respectively),²⁷ and the EAS of compound **1b** in 0.5 M KCl solution and its first-order derivative (*b*).

gously. Note that compound **2a** is insoluble in aqueous medium in the presence of KCl (or Na-CMC), probably, owing to smaller number of benzo-15-crown-5 moieties at the periphery of the macrocycle.²⁷ The presence of KCl in the system **1b**–Na-CMC causes the formation of a cofacial dimer; its EAS demonstrates a characteristic hypsochromic shift of the Q-band (this process is similar to that reported in Ref. 15). From the molar extinction coefficient value ($\epsilon = 7.7 \cdot 10^4$ L mol⁻¹ cm⁻¹) it follows that the dimer is the main particle (for monomer, one has $\epsilon = 1.47 \cdot 10^5$ L mol⁻¹ cm⁻¹). The reverse order of the addition of reactants, *viz.*, adding Na-CMC to a solution of heteronuclear complexes **1b**–KCl, does not lead to breakup of dimers. The use of NaCl instead of KCl also has no effect on the formation of particles. Thus, stability of the heteronuclear ionic sandwich complex [(**1b**)₂–(K⁺)_x–(Cl⁻)_x] suggests a high formation constant value, which favors dissolution of octa-crown-containing Pc in water in the presence of KCl.

The interaction between CTAB and crown-substituted Pc enables dissolution of compounds **1a,b** and metallo-

phthalocyanine **2a** (to a much lesser extent) with the formation of aggregates including cofacial heteronuclear dimers.* Solubilization of compound **1d** in the presence of CTAB also causes aggregation (Fig. 4, *a*, curve 2).²⁷ Figure 4, *b* presents the EAS of solutions of **1d**–SDS recorded at SDS concentrations from [SDS] \ll cmc (spectrum 1) to [SDS] \approx cmc (spectrum 5). The shape of the Q-band and position of its maximum in spectrum 5, as well as a comparison of this spectrum with the EAS recorded in dichloromethane (spectrum 6) are indicative of monomeric form of magnesium phthalocyaninate **1d** at [SDS] = $8.2 \cdot 10^{-3}$ mol L⁻¹. Compound **1b** in micellar solutions of SDS behaves analogously, whereas cobalt phthalocyaninate **2a** can exist in monomeric form only at [SDS] \gg cmc.^{27,30}

Taking metallophthalocyanine **1d** in microheterogeneous aqueous media containing lithium, sodium, and potassium dodecylsulfates as examples, it was shown that monomeric state of Pc is mainly formed in the presence of Na⁺ cation, which points to the need to provide the size correspondence between the benzo-15-crown ether cavity and the cation (see Table 1). When placed in micellar solutions of different surfactants, compound **1d** exists in different states, *viz.*, as monomer in the case of anionic surfactant SDS and mainly in aggregated form in the case of cationic surfactant CTAB (see Fig. 4, *a*).³¹

Thus, an analysis of aggregation of crown-containing Pc in aqueous solutions of surfactants whose polar "head" or counterion (cation) is much larger than the diameter of the crown ether cavity showed that hydrophobic interactions *per se* are insufficient for solubilization of compound **1d** in the micelle-bound monomeric state.

The behavior of metallophthalocyanine **1d** in aqueous SDS solutions was studied by electronic spectroscopy and by ¹H NMR spectroscopy including 2D ¹H–¹H correlation NOESY (Overhauser effect).³¹ The interacting protons in the molecule or in micelle-like molecular assemblies were determined and it was shown that compound **1d** exists in monomeric state at [SDS] \approx cmc and in the form of dimers and(or) bulkier aggregates at [SDS] $<$ cmc. Proton resonances from all SDS groups in the presence of metallophthalocyanine **1d** demonstrated upfield shifts relative to the SDS signals observed in the absence of Pc. The chemical shifts of methylene and methyl protons in the hydrocarbon chain of SDS {CH₃(CH₂)₁₁OSO₃Na} change to a greater extent than those of protons from the α - and β -CH₂ units adjacent to the polar "head" of the surfactant molecule. The results of 2D ¹H–¹H NOESY experiment suggest the interaction between aromatic protons and methylene protons from the {-(CH₂)₉-}

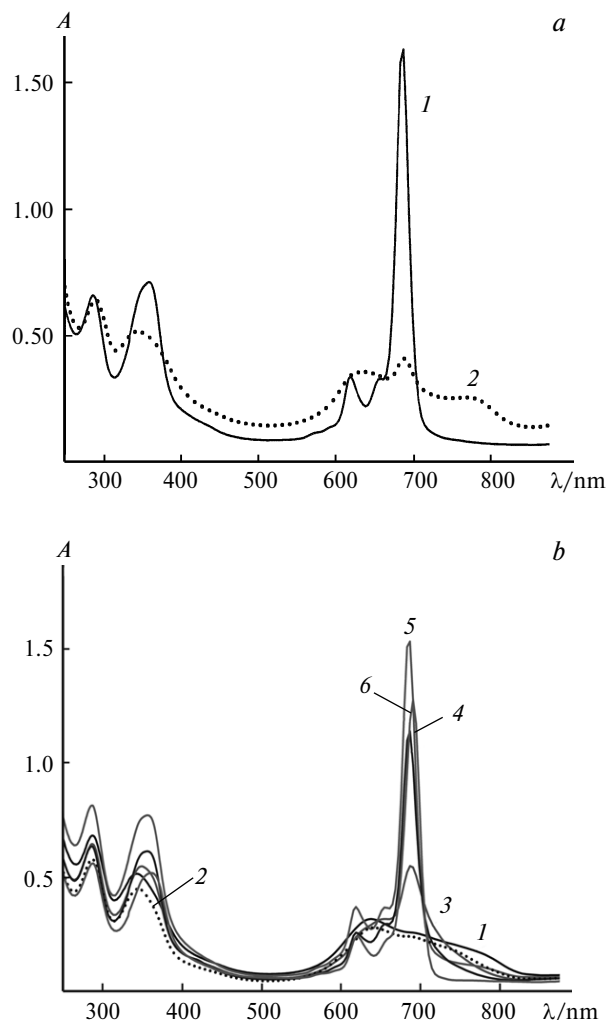


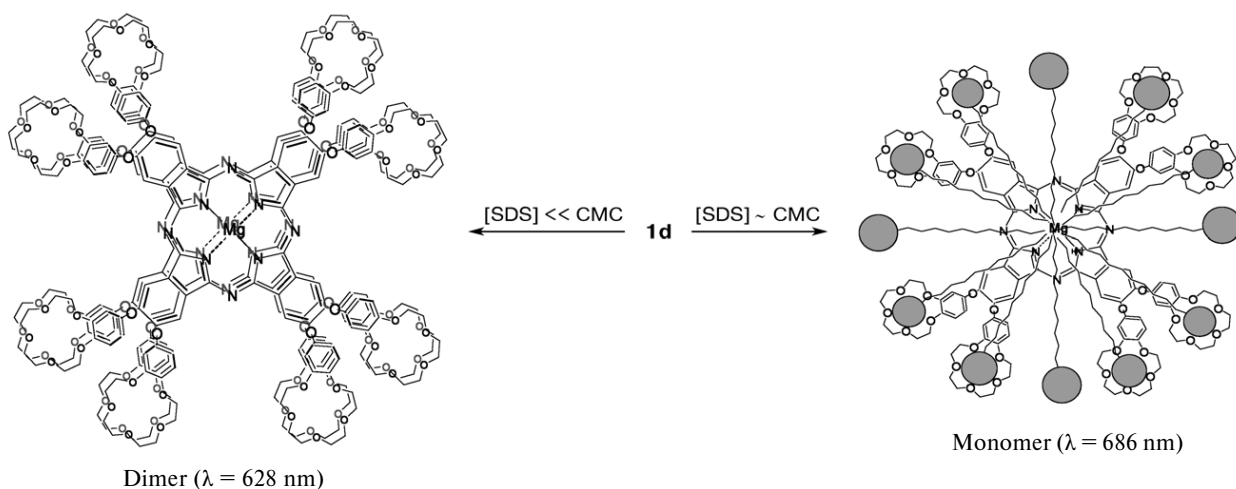
Fig. 4. Panel (*a*). Absorption spectra of compound **1d** in the presence of SDS (1) and CTAB (2) in aqueous medium³¹: [**1d**] = $9.2 \cdot 10^{-5}$ mol L⁻¹, [SDS] = $2.25 \cdot 10^{-2}$ mol L⁻¹ (1); [**1d**] = $1.1 \cdot 10^{-4}$ mol L⁻¹, [CTAB] = $8.6 \cdot 10^{-3}$ mol L⁻¹ (2).³¹ Panel (*b*). Absorption spectra of compound **1d** in the presence of SDS (1–5) in aqueous medium and in CH₂Cl₂ solution (6); [**1d**] = $8.8 \cdot 10^{-6}$ mol L⁻¹ (1–5), $7.7 \cdot 10^{-6}$ mol L⁻¹ (6); [SDS] = $0.46 \cdot 10^{-3}$ mol L⁻¹ (1), $1.85 \cdot 10^{-3}$ mol L⁻¹ (2), $5.1 \cdot 10^{-3}$ mol L⁻¹ (3), $6.9 \cdot 10^{-3}$ mol L⁻¹ (4), and $9.7 \cdot 10^{-3}$ mol L⁻¹ (5).

hydrocarbon chain of SDS in the system **1d**–CH₃(CH₂)₁₁OSO₃Na; therefore, compound **1d** mainly bound to the hydrophobic region of the micelle (Scheme 1).

Structural differences between surfactant molecules (SDBS, sodium bis(2-ethylhexyl)sulfosuccinate, or AOT, and SDC) specify the organization of molecule **1d** in microheterogeneous media.³² In aqueous SDBS solutions, metallophthalocyanine **1d** is in monomeric form at surfactant concentrations in the range of cmc₁–cmc₂ and in dimeric and(or) aggregated form at surfactant concentrations lower than cmc₁. According to NMR data obtained in that study, the binding between molecule **1d** and SDBS

* The CTAB polar "head" is about 5.8 Å in diameter; concentration [CTAB] = $8.6 \cdot 10^{-3}$ mol L⁻¹, which is much higher than the cmc in aqueous medium ($1.0 \cdot 10^{-3}$ mol L⁻¹).

Scheme 1



micelle is similar to that observed in the solubilization of this compound using SDS micelles.

Compound **1d** in direct (AOT–water) or reverse micelles (hexane–0.1 M aqueous AOT solution) is solubilized with the formation of dimers and (or) bulkier aggregates. Models for direct and reverse micelles in the form of monomer **1d**–SDS–H₂O (*a*) and aggregates **1d**–hexane–(AOT in H₂O) (*b*) are presented in Fig. 5.

Polar cavity including the micelle water pool and the hydrophilic surface layer of polar groups of a surfactant is an important component of the structure of reverse micelles. The radius of micelle water pool is evaluated using the formula³³

$$R = (3V_w/a_0)w_0 + 3V_h/a_0,$$

where $V_w = 30 \text{ \AA}^3$ is the volume of water molecule, V_h is the volume of the polar region of the surfactant molecule, a_0 is the surface area per surfactant molecule at the water–

oil interface, and w_0 is the solvent-to-surfactant concentration ratio.

For AOT ($a_0 = 66 \text{ \AA}^2$, $V_h = 222 \text{ \AA}^3$, $w_0 = [\text{H}_2\text{O}]/[\text{AOT}] = 9$) the calculated diameter of the micelle water pool ($\sim 44 \text{ \AA}$) exceeds the diameter of molecule **1d** ($\sim 30 \text{ \AA}$) evaluated by the method of molecular mechanics (MM3) using the CAChe WorkSystem Pro 6.0 software. It follows that in the case of reverse micelles molecules **1d** are solubilized and enter the micelle water pool with the formation of a complex between the Na⁺ cation of AOT and the crown ether moiety. Since hydrophobic groups of AOT in the reverse micelle are in the organic phase, they do not preclude stacking aggregation of phthalocyaninate **1d** in the micelle water pool (see Fig. 5, *b*).³²

Polyelectrolytes. The behavior of compounds **1a** and **1d** in organized microheterogeneous systems suggests that monomerization of Pc in aqueous solutions is influenced

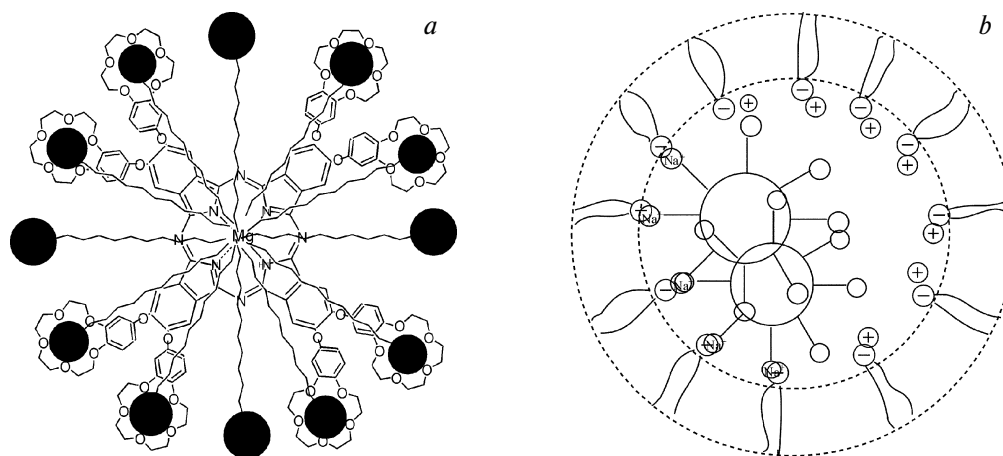


Fig. 5. Cross-sectional models for direct (*a*) and reverse micelles (*b*) with solubilized magnesium phthalocyanine **1d**. Black solid circles denote Na⁺–O₃SO–(SDS) groups, large and small open circles denote the macrocycle and crown ether fragments of metal-phthalocyanine **1d**, respectively; and wavy lines denote hydrophobic radicals.

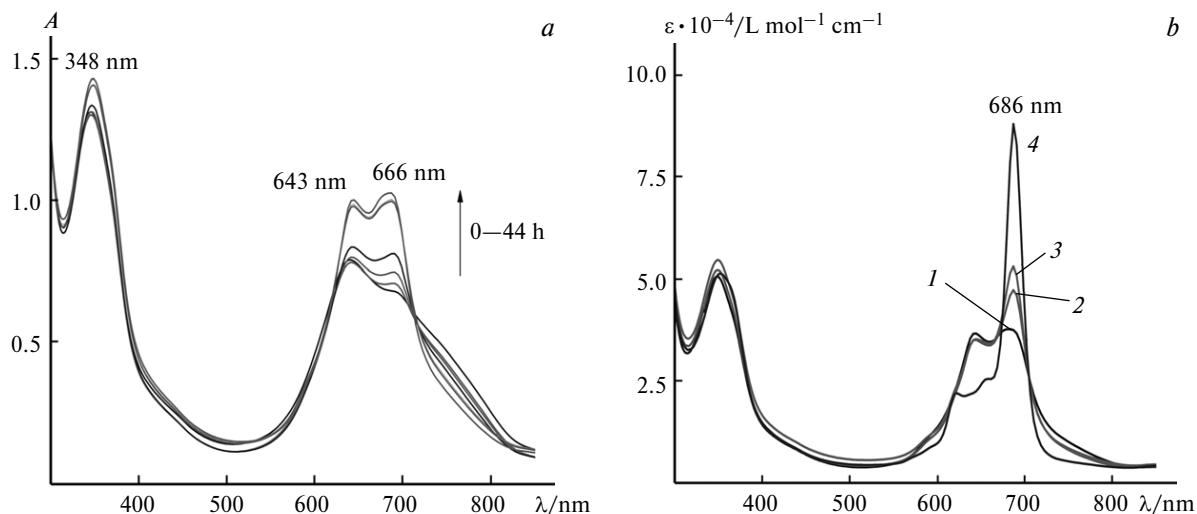


Fig. 6. Changes in the EAS of the system **1d**–PSS (water, [PSS] = const) with time (*a*) and in the absorption spectra (*b*) of aqueous solution of the system **1d**–PSS (*1*) in the presence of SDC (*2*, *3*) and SDC + NaCl (*4*). Concentration/mol L⁻¹: [**1d**] = $1.54 \cdot 10^{-5}$, [PSS] = $2.1 \cdot 10^{-2}$, [SDC] = $4.76 \cdot 10^{-3}$, and [NaCl] = $9.2 \cdot 10^{-2}$.³⁴

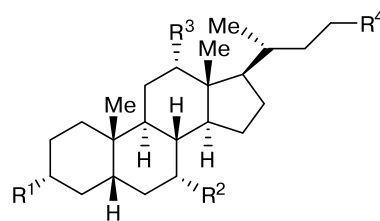
by the structure and charges of anionic surfactants and polyelectrolytes.³⁴ Figure 6, *a* demonstrates how the EAS of aqueous solution containing aggregated metallophthalocyanine **1d** and the simplest polyelectrolyte sodium poly(styrene sulfonate), or PSS, changes with time. If in the case of anionic surfactants SDS and SDBS compound **1d** exists in monomeric state in micellar solutions,^{31,32} utilization of SDC and PSS requires that the ionic strength of the solution be increased by, *e.g.*, adding NaCl. For PSS, subsequent addition of surfactants, for instance, SDC, favors a considerable increase in the proportion of monomeric **1d** (Fig. 6, *b*, curve *4*).

Earlier,³⁵ encapsulation of Na⁺ ions was demonstrated by ¹H NMR spectroscopy taking Pc with annelated crown-5 moieties in organic solvent as examples. The formation of supramolecular guest–host complex upon coordination of Na⁺ ion to the crown ether macrocyclic cavity of compound **1d** followed by the onset of electrostatic interaction between oppositely charged Pc and PSS favors transfer of metallophthalocyanine **1d** from the aqueous phase to the hydrophobic region of polyelectrolyte. Joint action of these interactions underlies the existence of compound **1d** in monomeric form in aqueous PSS solution and subsequent increase in the concentration of the monomer upon adding NaCl and SDC (see Fig. 6, *b*), which is confirmed by an increase in the fluorescence intensity. Simultaneous presence of PSS and SDC has a synergistic effect.³⁴

Specific features of solubilization of crown- and phosphoryl-substituted phthalocyanines in bile salt solutions

Bile salts are natural steroid micelle-forming compounds. Unlike traditional surfactants with long hydro-

phobic alkyl radicals and small polar groups, BS are characterized by planar diphlicity.^{36–38} The structures of the best known BS, *viz.*, sodium cholate (SC), sodium deoxycholate (SDC), sodium taurocholate (STC), and sodium taurodeoxycholate (STDC) are presented below.



Compound	R ¹	R ²	R ³	R ⁴
SC	OH	OH	OH	CO ₂ Na
SDC	OH	H	OH	CO ₂ Na
STC	OH	OH	OH	CONH(CH ₂) ₂ ·SO ₃ Na
STDC	OH	H	OH	CONH(CH ₂) ₂ ·SO ₃ Na

The number of hydroxyl groups and their orientation relative to the steroid skeleton causes a variety of hydrophobic–hydrophilic properties of BS. Asymmetric structure and multiple noncovalent interactions including hydrogen bonds between OH groups of different molecules allow the BS molecules to form hierarchical structures (primary, secondary, tertiary and guest–host assemblies) in crystals similarly to proteins. Numerical values of the intensity ratio of the first and third vibronic peaks (I_1/I_3) in the fluorescence emission spectrum of pyrene, which are used for characterization of the medium polarity, show that pyrene molecules in micellar solutions of BS are in non-polar (hydrocarbon) local environment. The environment is more hydrophobic in the case of SDC and STDC (Table 3).

The presence of eight crown-containing substituents in the molecule and the possibility of axial coordination

Table 3. Properties of selected bile salts

BS	cmc'	cmc''	cmc'''	I_1/I_3
	mmol L ⁻¹			
SC	7.78	8.25	5.41 ⁴⁰	0.88
SDC	3.80	5.36	1.18 ⁴¹ , 1.68 ⁴⁰	0.69
STC	6.68	7.30		0.94
STDC	1.88	2.62		0.71
				1.96

Note. cmc' was determined from measurements of surface tension in water³⁹, cmc'' was determined from conductivity in water³⁹, cmc''' was determined in 0.1 M NaCl solution; I_1/I_3 is the intensity ratio of the first and third vibronic peaks in the fluorescence emission spectrum of pyrene in water at 20 °C.

involving magnesium ion at the center of the macrocycle⁴² favors dissolution of metallophthalocyanine **1d** in water and is accompanied by the appearance of a broad band in the EAS in the range of 630–750 nm, thus indicating an aggregated state of Pc (Fig. 7, spectrum 1). Similarly to the spectrum of magnesium phthalocyaninate **1d** in micellar solutions of SDC⁴³ the EAS of **1d** in the presence of SC also changes (spectrum 2).⁴⁴ The addition of NaCl to the system **1d**–SC causes an increase in the optical density of the Q-band and the appearance of an isosbestic point on the long-wavelength side (spectra 3–5). Zinc phthalocyaninate **1e** behaves analogously. The absorption spectra of the solutions **1d**–BS correspond to partial or

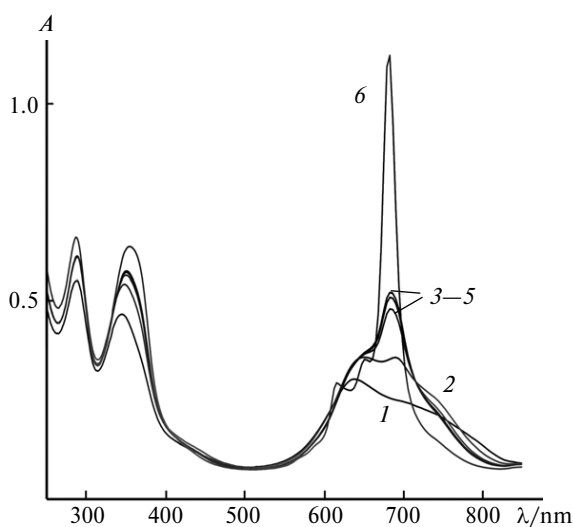


Fig. 7. Absorption spectra of aqueous solutions of the systems **1d** (1), **1d**–SC (2), **1d**–SC–NaCl (3–5), and **1d**–SC–NaCl–SC (6); [**1d**] = $9.33 \cdot 10^{-6}$ mol L⁻¹ (1–6); [SC] = $9.9 \cdot 10^{-3}$ mol L⁻¹, [SC] : [**1d**] = 1060 (2); [SC] = $9.9 \cdot 10^{-3}$ mol L⁻¹, [NaCl] = 0.123 mol L⁻¹, [SC] : [**1d**] = 1060 (3–5); and [SC] = $38.45 \cdot 10^{-3}$ mol L⁻¹, [NaCl] = 0.123 mol L⁻¹, [SC] : [**1d**] = 4126 (6)⁴⁴.

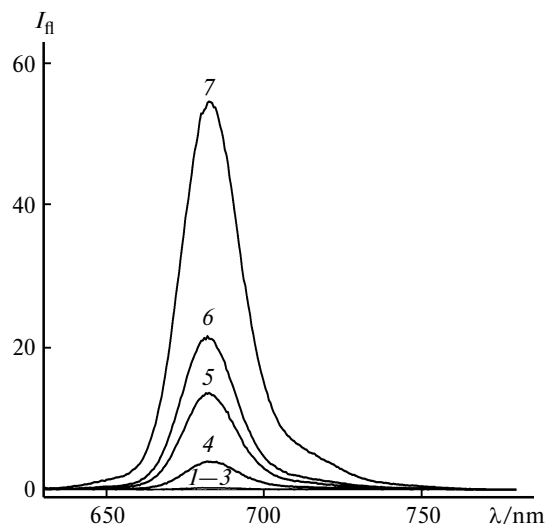


Fig. 8. Influence of SDC concentration (1–6) and NaCl added (7) on the fluorescence intensity of metallophthalocyanine **1d** in aqueous micellar solutions of SDC; [**1d**] = $2.76 \cdot 10^{-6}$ mol L⁻¹, [SDC] = $(0-4.8) \cdot 10^{-3}$ mol L⁻¹ (1–3), $6.7 \cdot 10^{-3}$ mol L⁻¹ (4), $1.2 \cdot 10^{-2}$ mol L⁻¹ (5), $1.76 \cdot 10^{-2}$ mol L⁻¹ (6), $1.76 \cdot 10^{-2}$ mol L⁻¹, and [NaCl] = 0.1 mol L⁻¹ (7).⁴³

nearly complete (spectrum 6) monomerization of Pc, which depends on the concentration of SDC and on the ionic strength of the solution. Phthalocyanine **1a** can also be dissolved in aqueous SDC solution; however, its absorption spectra correspond to mainly aggregated state of Pc both without and in the presence of SDC and NaCl.³⁴

Fluorescence appears only upon adding SDC to the solution of compound **1d**. The fluorescence intensity increases with the concentration of SDC and reaches a maximum value at [SDC] \gg cmc in the presence of NaCl (Fig. 8).⁴³ This confirms the conclusion that an increase in the ionic strength of the solution and in the SDC concentration leads to monomerization of metallophthalocyanine **1d** in micellar solutions of SDC since H-aggregates of phthalocyanines do not fluoresce.

The optical density of compound **1d** ([**1d**] = const) is plotted vs. surfactant concentration in aqueous micellar solutions of SDS and SDC in Fig. 9.^{31,43} In the microheterogeneous system SDS–**1d**, the optical density of the solution initially increases and then remains constant in the range of cmc₁–cmc₂. Metallophthalocyanine **1d** present in the solution exists as micelle-bound monomer (extinction coefficient $\epsilon = 1.8 \cdot 10^5$ L mol⁻¹ cm⁻¹; see curve 1).

In the system containing SDC, the optical density of aqueous solution of compound **1d** increased with the surfactant concentration even at [SDC] \gg cmc (see Table 2 and Fig. 9, curve 2). Spectral data for the solutions **1d**–SDC were processed using the Benesi–Hildebrand method^{44,45} in the coordinates $1/(A-A_0)$ and $1/[SDC]^2$. The formation constant of the **1d**·2SDC aggregate is close to a value of 400 L² mol⁻², as was expected for SDC.^{36–38}

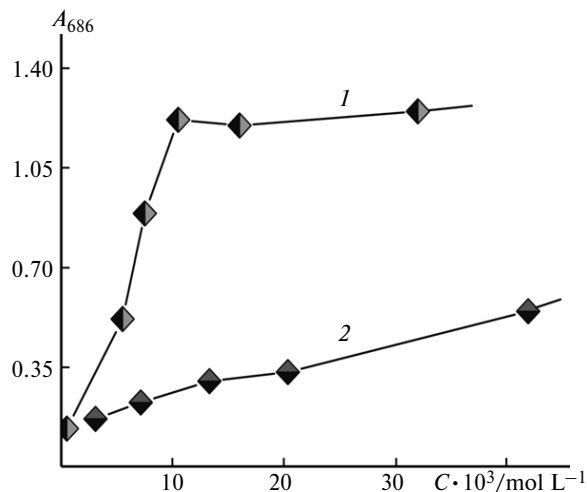


Fig. 9. Optical density of solutions of magnesium phthalocyaninate **1d** plotted vs. concentration of SDS (1) and SDC (2) at $\lambda = 686 \text{ nm}$.^{31,43}

Having reached the cmc value, the diameter of spherical SDS micelles remains almost unchanged, whereas the average size of SDC aggregates (micelles) monotonically increases with the surfactant concentration. Sodium deoxycholate micelles are characterized by much smaller aggregation numbers (N_{agg}) and higher polydispersity compared to SDS micelles.^{37,38} At $[\text{SDC}] \sim 50 \cdot 10^{-3} \text{ mol L}^{-1}$, the average N_{agg} value ranges from two to five molecules; however, N_{agg} can be as high as 20 molecules at $[\text{SDC}] > 0.1 \text{ mol L}^{-1}$.⁴⁶

Zinc phthalocyaninate **4** bearing phosphonate peripheral substituents is almost insoluble in water, being, however, soluble in the phosphate buffer (PBS, pH 7.4).⁴⁴ Based on the results of potentiometric titration of 1,5-bis-[2-(oxyethoxyphosphoryl)-4-ethylphenoxy]-3-oxapentane⁴⁷ with phosphoryl-containing fragments, one can assume that compound **4** forms a multiply charged anion in PBS. The position of the Q-band in the EAS of this phthalocyaninate ($\lambda_{\text{max}} = 644 \text{ nm}$) suggests that it mainly exists in the form of H-dimers (Fig. 10, spectrum 1).⁴⁴ In organized microheterogeneous media (supramolecular assemblies) containing oppositely charged surfactants ($[\text{surfactant}] > \text{cmc}$) phthalocyaninate **4** exists as monomer, which is confirmed by its EAS recorded in the presence of cationic surfactant CTAB (spectrum 2) and anionic surfactant SDC (spectrum 3). The absorption spectrum of **4** in micellar solutions of CTPB obeys the same pattern as the spectrum of the system **4**–CTAB (see Fig. 10, spectrum 2). The cmc values for CTAB and CTPB in water are $1.0 \cdot 10^{-3}$ and $0.16 \cdot 10^{-3} \text{ mol L}^{-1}$, respectively: the lower the cmc the more stable the micelles.⁴⁸ The $\lg \epsilon$ values for the systems **4**–CTAB–PBS and **4**–SDC–PBS are 5.37 and 5.16, respectively. Experimental spectra of micellar solutions of **4**–CTAB and **4**–SDC in PBS can be represented by the sums of three and four components

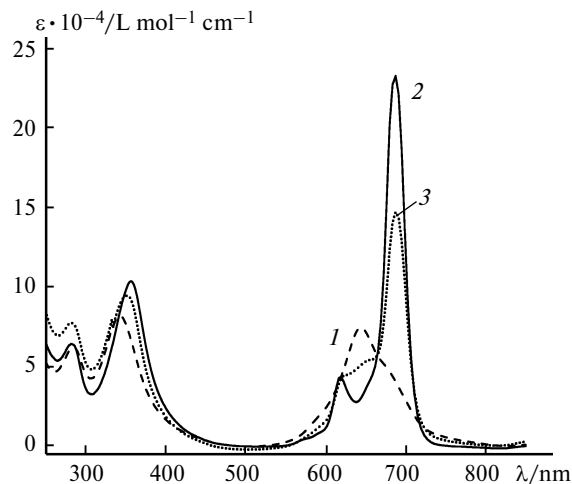


Fig. 10. Absorption spectra of zinc phthalocyaninate **4** in phosphate buffer PBS (1) and in microheterogeneous media "cationic surfactant (CTAB)–PBS" (2) and "anionic surfactant (SDC)–PBS" (3); $[\mathbf{4}] = 6.31 \cdot 10^{-6} \text{ mol L}^{-1}$.⁴⁴

characterized by $r^2 = 0.9976$ (for **4**–CTAB) and $r^2 = 0.9974$ (for **4**–SDC). The optical density ratio of the components corresponding to the vibronic peaks, A_{653}/A_{620} (for **4**–CTAB) and A_{652}/A_{624} (for **4**–SDC), is 0.837 and 0.925, respectively. The last-mentioned value suggests that compound **4** exists in the micellar solution containing SDC not only as monomer, but also as H-dimer.⁴⁴

Peculiar features of solubilization of zinc phthalocyaninate **4** were studied using solutions of SDS and BS (SC, SDC, taurine-conjugated STC and STDC). The anionic surfactants SDS and BS differ in the structure of micelles and in the number of the micelle-forming surfactant molecules.⁴⁴ In PBS, specific features of BS had almost no effect on the EAS of compound **4** in the microheterogeneous medium. The spectra of the systems **4**–BS–PBS were characterized by close values of the extinction coefficient for the Q-band and demonstrated some features that were mentioned above for the spectrum of the system **4**–SDC–PBS (see Fig. 10). Moreover, the number of components and the component area ratio in the experimental spectrum of the system **4**–SDS–PBS are close to those found for the system **4**–SDC–PBS. At constant SDC concentration, the degree of aggregation of phthalocyaninate **4** increased with its concentration, while the difference between the first-order derivatives on the short-wavelength side of the Q-band pointed to a noticeable contribution of the aggregation of phthalocyaninate **4**. In the dark, the spectral pattern remains unchanged for a long period of time. In diffuse light, when compound **4** was stored in the form of a monomer of multiply charged anion $\{\text{group} -\text{P}(\text{O})(\text{OC}_5\text{H}_{11})\text{O}^-\}$ in the microheterogeneous medium "anionic surfactant–PBS" ($[\text{surfactant}] > \text{cmc}$) the optical densities of the systems **4**–surfactant–PBS decreased in the order $\mathbf{4}\text{--SDS} > \mathbf{4}\text{--SDC} \approx \mathbf{4}\text{--SC} \approx \mathbf{4}\text{--STC}$.⁴⁴

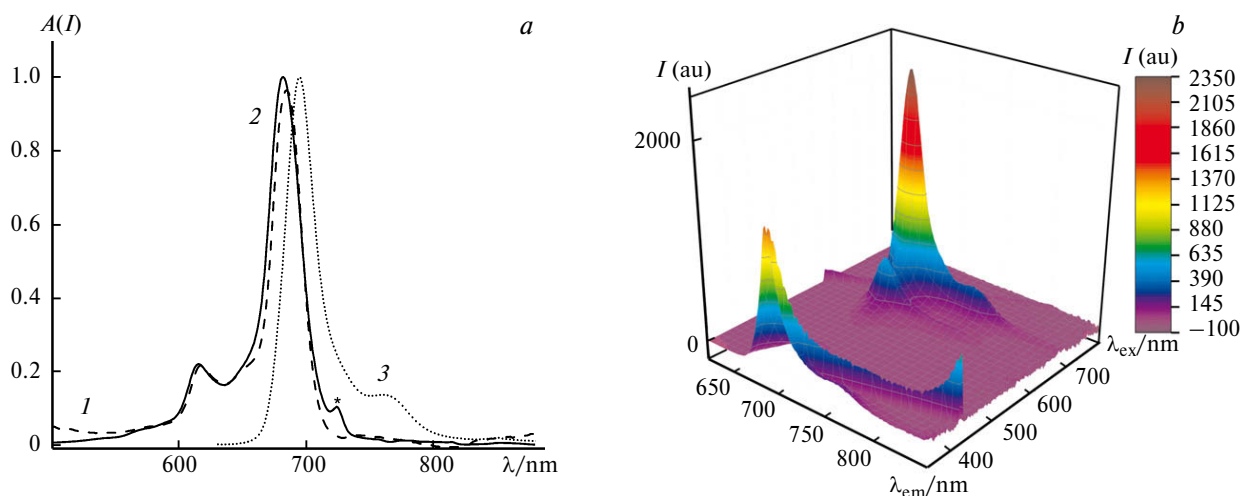


Fig. 11. Panel (a). Normalized absorption spectra (I), excitation spectra ($\lambda_{\text{em}} = 725$ nm, 2) and fluorescence spectra ($\lambda_{\text{ex}} = 620$ nm, 3) of the system 4–SDC–PBS. The asterisk denotes the artifact appeared upon photoexcitation of the Pc molecules at λ_{em} . Panel (b). 3D representation of the excitation–fluorescence matrix (in the coordinates I and λ_{em} , λ_{ex}) for the system 4–SDC–PBS.⁴⁴
Note. Figures 11 and 19 are available in full color on the web page of the journal (<https://link.springer.com/journal/volumesAndIssues/11172>).

In PBS, phthalocyaninate **4** exists in the aggregated state and does not fluoresce similarly to the components of the medium (PBS, SDS, BS). The normalized absorption, excitation, and fluorescence spectra, as well as the 3D representation of the excitation–fluorescence matrix for the system 4–SDC–PBS are shown in Fig. 11. As can be seen, the excitation spectrum of phthalocyaninate **4** (see Fig. 11, a, spectrum 2) repeats the absorption spectrum (spectrum 1), while the fluorescence spectrum (spectrum 3) undergoes a bathochromic shift relative to the absorption spectrum. The excitation–fluorescence matrix obtained (see Fig. 11, b) to a good accuracy corresponds to the product of the excitation and fluorescence spectra of phthalocyaninate **4** at their maxima without noticeable features observed.⁴⁴

The Stokes shift is 10 nm for the system 4–SDC–PBS and 10.5 nm for the system 4–SDS–PBS. The excitation and fluorescence spectra of phthalocyaninate **4** in the microheterogeneous media based on SC, STC and STDC, and SDS exhibit no noticeable changes compared to the spectra of the system 4–SDC–PBS. Therefore, the known differences in the hydrophobic–hydrophilic properties of BS have almost no effect on the EAS and fluorescence spectra of compound **4** ($\lambda_{\text{max}}^{\text{em}} = 692$ nm). The fact that the structure of BS has little impact on the EAS and fluorescence of phthalocyaninate **4** can be interpreted as follows: solubilization of **4** occurs in those regions of the BS micelles that are close in polarity (Fig. 12).³⁸ Figure 12 illustrates the sequence of BS aggregation in aqueous medium and encapsulation of guest molecules in their

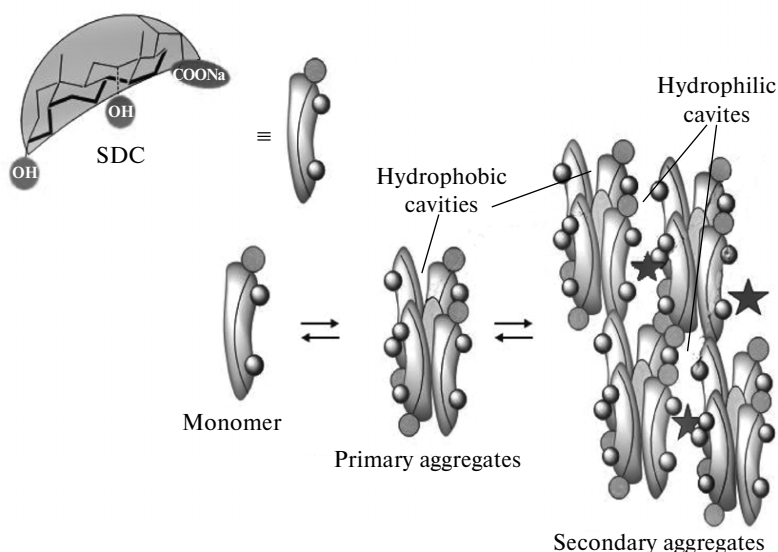


Fig. 12. Aggregation of SDC in aqueous medium and binding guest molecules in SDC cavities.

cavities. The BS micelles and aggregates have small unfilled cavities. In small micelles, these cavities are rather hard and hydrophobic, being of higher polarity, softer, and relatively capacious in large micelles. Nonpolar cavities of BS micelles can solubilize hydrocarbon molecules, while polar bulky guest molecules are encapsulated in the BS aggregates. Solubilization of the pentyl groups of compound **4** in hydrophobic cavities of the BS micelles can be one of those opportunities.

How the method of introducing crown ether moieties and the number of crown ether groups influences solubilization of phthalocyanines

Supramolecular assembly of tetra-15-crown-5-phthalocyanines containing crown ether moieties annelated with benzene rings in organic media has been thoroughly studied.¹² The solubility of compounds and their supramolecular association depends strongly on the nature of the complex-forming metal and solvent. For instance, an indium(III) complex [(15C5)₄Pc]In(OH) is soluble in CHCl₃ and DMSO (biocompatible solvent of low toxicity) and exists in the monomeric state (Q-band maximum is at $\lambda = 696$ nm), whereas dissolution of this complex in methanol causes its aggregation with the formation of a cofacial ($\pi-\pi$) H-dimer⁴⁹ similarly to the Pc containing substituents attached to the macrocycle *via* an oxygen spacer. A corresponding complex of magnesium phthalocyaninate **3** [(15C5)₄Pc]Mg is much more poorly soluble in nonpolar solvents, being insoluble in polar and aqueous media owing to pronounced tendency to stacking interactions.

In spite of a large number of studies on supramolecular assemblies formed in solution as a result of cation-induced aggregation of macrocycles,^{11,12} the structure of supramolecular aggregates was proved by X-ray diffraction only once. Namely, the addition of an excess of a methanol solution of rubidium nicotinate to a solution of hydroxyaluminum phthalocyaninate [(HO)Al(15C5)₄Pc] in CHCl₃ resulted in the supramolecular dimeric complex [(μ -oxo)bis(tetra-15-crown-5-phthalocyaninate)(nicotinate)aluminum(III)]tetra(rubidium)bis(nicotinate)]. Single crystals of the complex were isolated for the first time. An X-ray study of {[Rb₄(NicAl(15C5)₄Pc)₂(μ -O)]²⁺(Nic⁻)₂} • 2.36HNic • 11H₂O showed that two Pc molecules are linked by the Al—O—Al bridge, thus forming a sandwich structure involving the crown moieties and rubidium cations.⁵⁰

The magnesium complex [(15C5)₄Pc]Mg **3** is insoluble in water, but can be solubilized in microheterogeneous aqueous media of synthetic anionic surfactants (SDS and SDBS) with the formation of monomers (lg $\epsilon_{681} = 5.07$ and lg $\epsilon_{682} = 5.1$, respectively).⁵¹ Micellar solutions of the monomers, just like solutions of other phthalocyanines (see, *e.g.*, Ref. 34), bleach when stored in the light. The

process is not accompanied by the appearance of new bands in the EAS in the visible range.

Interestingly, irrespective of the number and addition fashion of the crown ether fragments, compounds **1d**, **2b**, and **3** containing Mg²⁺ as the complex-forming metal exist in the monomeric state in solutions of traditional anionic surfactants (SDS and SDBS). However, the solubilization efficiency of the biocompatible STDC toward magnesium phthalocyanines bearing different number (four and eight) of (15-crown-5) moieties in peripheral substituents or annelated with the macrocycle, changes in the order **1d** >> **2b** > **3**.⁵¹ Therefore, magnesium phthalocyaninate **3** is the most sensitive to the structure of the micelle-forming surfactant. Different state of compound **3** in the organized microheterogeneous media based on SDS and STDC is illustrated in Fig. 13.⁵¹ An analysis of the behavior of magnesium phthalocyanines **1d**, **2b**, and **3** in micellar solutions of BS shows that molecular organization of crown-substituted Pc varies from mainly monomeric state for compound **1d** to aggregated state for magnesium phthalocyaninate **3**.

Aggregation of metallophthalocyanine **3** can occur through both stacking interaction between the phthalocyanine moieties and hydrogen bonding between water molecules axially coordinated to the magnesium ion and crown ether substituents.⁵² Higher tendency of compound **3** to aggregation can be explained by the almost planar structure and the absence of large steric hindrances to intermolecular interactions. Rather, in complexes **1d** and **1b** the benzo-crown ether groups should be arranged nearly perpendicular to the phthalocyanine macrocycle plane and thus preclude intermolecular stacking interactions.⁵³ At the same time, the type of self-organization of BS in aqueous solutions, the rigid steroid skeleton, and the shape of the macrocycle can influence the solubilization process

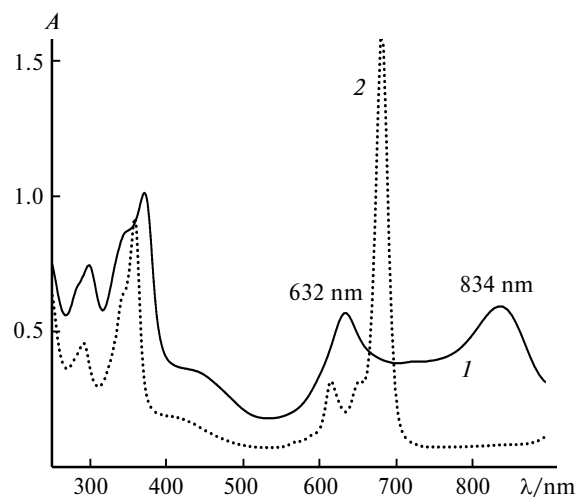


Fig. 13. Electronic absorption spectrum of compound **3** in micellar solutions of STDC (**1**) and SDS (**2**).⁵¹

and the formation of micelle-bound Pc monomers. In particular, the shape and size of guest molecules to a great extent determine the arrangement of the surrounding host (BS) molecules, *viz.*, micelles and BS aggregates are mutually adjustable supramolecular objects.⁵⁴

The state of phthalocyanine **1a** in solutions of water-soluble derivatives of fullerene C₆₀ and amphiphilic polymer — polyvinylpyrrolidone

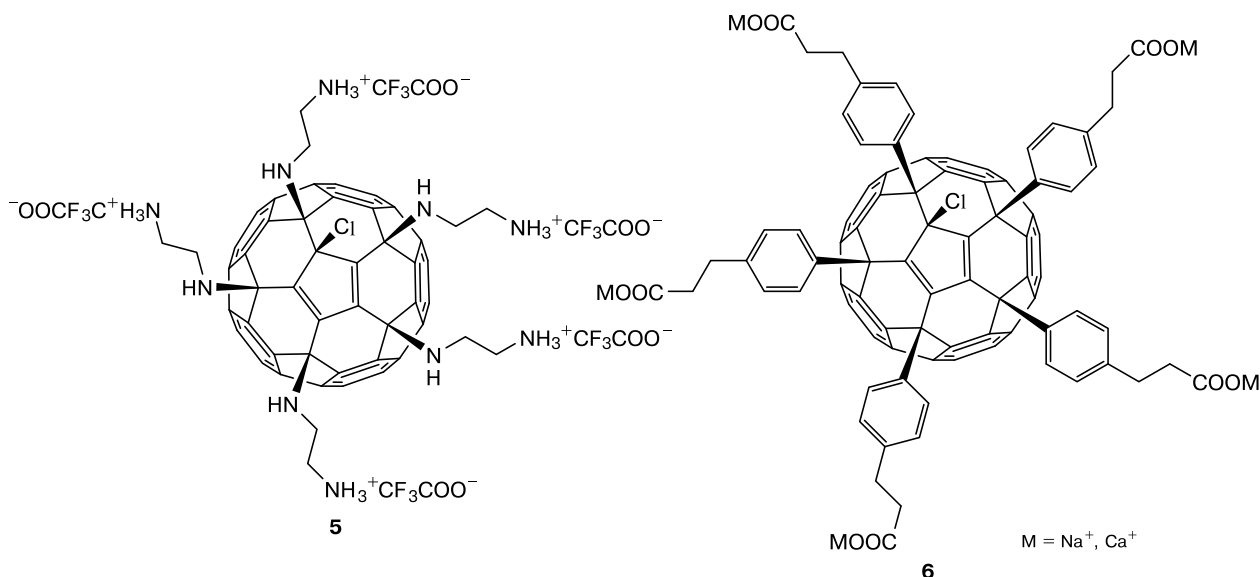
Water-soluble derivatives of fullerene C₆₀ bearing five ligands attached to the same fullerene hemisphere (compounds **5** and **6**) in accordance with the cyclopentadienyl motif were for the first time used as solubilizing agents nearly a decade ago.⁵⁵ They can be treated as surfactant-like compounds whose hydrophobic region represents a rigid sphere built of carbon atoms rather than flexible hydrocarbon chains typical of conventional surfactants. The hydrophilic fragment of these molecules is formed by attaching ligands with changed functional groups (NH₃⁺ and COO⁻) to the fullerene. Considering the charge carried, compounds **5** and **6** can be classified as cationic and anionic surfactant, respectively. It was for the first time demonstrated⁵⁵ that the use of these systems as solubilizing agents causes dissolution of phthalocyanine **1a** in water. The process can probably be favored by the formation of hydrogen bonds N—H---O(CH₂) and by coordination of cations within the crown ether cavities in compound **1a**. However, unlike the behavior of compound **1a** in the micellar solutions of SDS at [SDS] ≈ cmc, solubilization of the phthalocyanine in the presence of compounds **5** and **6** is not accompanied by its monomerization in solution. It should be noted that the presence of —COONa group in the fullerene-containing compound **5** does not preclude stacking aggregation of phthalocyanine

1a in solution. In the case of conventional anionic surfactant with Na⁺ as counterion (*e.g.*, SDS) and crown-containing Pc solubilization of phthalocyanine at [surfactant] ≈ cmc is accompanied by its monomerization due to the synergistic effect of guest—host interactions, electrostatic and hydrophobic processes (see above).

Magnesium phthalocyaninate **1d** exists in the aggregated form in neat water, phosphate buffer, and aqueous solutions of Triton X-100 and polyvinylpyrrolidone (PVP) (~2%).⁵⁶ Aggregated state is also characteristic of zinc phthalocyaninate **1e** in the PBS—PVP solution (0.6 wt.% PVP). The two phthalocyaninates have similar EAS in PVP. Compound **4** in PBS exists in the dimeric state (see Fig. 10)⁴⁴ and goes to nearly monomeric state in the presence of PVP (Q-band parameters: λ_{max} = 692 nm, lgε_{max} = 5.20). It also behaves in a similar fashion in aqueous solutions of Pluronic F127. The Q-band maximum in the EAS of compound **4** in aqueous PVP solution undergoes a bathochromic shift relative to the EAS maximum in DMSO solution. Both the EAS of compound **4** in solutions of amphiphilic polymers and their comparison with the EAS of the metal-free Pc recorded under identical conditions are indicative of the effect of pentyl group and the central zinc ion on the degree of monomerization.

Microheterogeneous systems containing metallophthalocyanine **1d**: a small-angle X-ray scattering study

Solutions of Pc and processes responsible for the changes in the EAS (from suspension to true solution) were studied by small-angle X-ray scattering (SAXS).⁵⁷ Using the electronic spectroscopy and SAXS data, it was shown that freshly prepared solutions of compounds **1a**,



1d, and **1e** (concentration: 10^{-4} mol L $^{-1}$ in 0.5 M KCl solution) contain particles nearly 25 nm in size. Depending on the complex-forming metal and on the initial state of the sample, the formation of a true solution in 0.5 M aqueous KCl containing H-dimers of the compounds under study¹⁵ takes more than two weeks. For instance, the particle size of compound **1a** changed from 43 to 1–2 nm in the course of dissolution. The state of microheterogeneous phthalocyanine-containing systems based on PSS was also studied by SAXS.³⁴ Almost no SAXS was observed for metallophthalocyanine **1d** whose absorption spectrum corresponds to an aggregated, stable, and non-fluorescent state. This result agrees with the published data⁵⁷ and confirms the formation of a true solution. Samples of spectrally characterized systems (aqueous solutions of PSS, PSS–NaCl, and **1d**–PSS–NaCl) demonstrated weak scattering (Fig. 14), which led to relatively large errors in the determination of quantitative parameters and difficulties in assessing the shape macromolecules. The Guinier plot $\lg(I) - q^2$ (I is the scattering intensity, q is the scattering vector $4\pi \sin \theta / \lambda$, where θ is the angle and λ is the wavelength) has a linear portion indicative of the presence of monodisperse particles. The gyration radius R_g (structural characteristic of a polymer chain in solution) systematically increases in the order PSS, PSS–NaCl, **1d**–PSS–NaCl, being equal to 1.3, 1.4, and 1.5 nm, respectively. Assuming monodispersity of the scattering particles, one can assess their shape from the slope of the scattering curve plotted in the double logarithmic scale. On the one hand, scattering objects with a shape intermediate between a rod (cylinder) and a disk can be present in the solution. On the other hand, water is a good solvent for polymeric electrolytes and therefore (especially, for the system **1d**–PSS–NaCl) the shape of the scattering particles can be close to elongated swollen (hydrated) coils (rings, reels) whose exponent equal to 5/3 is close to that observed in the SAXS experiment.³⁴

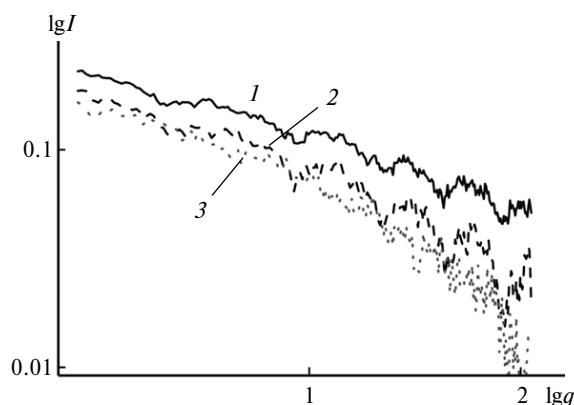


Fig. 14. Small-angle X-ray scattering curves of the samples PSS (**1**), PSS–NaCl (**2**), and **1d**–PSS–NaCl (**3**) in the double logarithmic scale after subtraction of the buffer. Oscillations are an artifact resulting from low measurement statistics.³⁴

Almost no SAXS was observed from the microheterogeneous systems based on SDC–**1d**.⁴⁴ It follows that there are no noticeable concentrations of nanoparticles or that the nanoparticle size much exceeds the resolution of the instrument used (65 nm). There is a clearly seen correlation peak indicating a certain degree of ordering in the system; the peak intensity increases with the SDC concentration.⁵⁸ Metallophthalocyanine **1d** is present in solutions of SDC in the form of micelle-bound monomer; at $[\text{SDC}]/[\mathbf{1d}] > 1000$, a new scattering center can appear.⁴³ However, its concentration was much lower than that of the unfilled (hollow) SDC micelles.

An attempt to determine the hydrodynamic diameter (D_h) of particles in the microheterogeneous system **1d**–SDBS using dynamic light scattering also failed.³² For SDBS, one has $D_h = 4.2$ nm,²³ which falls in the range of values typical of spherical micelles.²⁰ Solubilization of phthalocyaninate **1d** causes the diameter of SDBS micelle to increase by about 0.4 nm only, which, probably, is determined by the ratio of the hollow and phthalocyanine-loaded micelles. The zeta-potential of the SDBS micelles formed (from –70 to –73 mV) was close to the characteristic values (from –60 to –75 mV), being independent of the presence of phthalocyaninate **1d**. The high negative zeta-potential value is indicative of the stability of the micellar solutions. Indeed, the EAS of aqueous micellar solutions of **1d** in the presence of anionic surfactants (SDBS, SDS) remain unchanged for a long period of time provided that no photobleaching occurs (see above). Thus, experiments with anionic surfactants (SDC, SDBS) at their concentrations exceeding the cmc only confirmed the microheterogeneity of the media containing solubilized metallophthalocyaninate **1d** in the micelle-bound monomeric state.

Supramolecular, fluorescence-active phthalocyanine-containing hydrogels based on sodium deoxycholate

Similarity between the properties of synthetic gels and living tissues, such as high water uptake, reversibility, biocompatibility, the ability to retain an active component, transfer it, and release upon external stimuli underlies intensive research into gelation including processes involving small molecules (see, *e.g.*, Refs 37, 38, 59–61 and references cited therein).

The "building blocks" of supramolecular gels based on small molecules include surfactants and amino acids.^{38,62,63} The formation of low-molecular-weight hydrogels (Fig. 15, *a*) based on natural compounds (SDC and lysine hydrochloride, Lys·HCl) in the presence of metallophthalocyanine **1d** as active component was studied.^{43,56} The micelle-forming properties of SDC allowed compound **1d** to embed into supramolecular gels. According to the EAS, compound **1d** in the gels is mainly in the aggregated

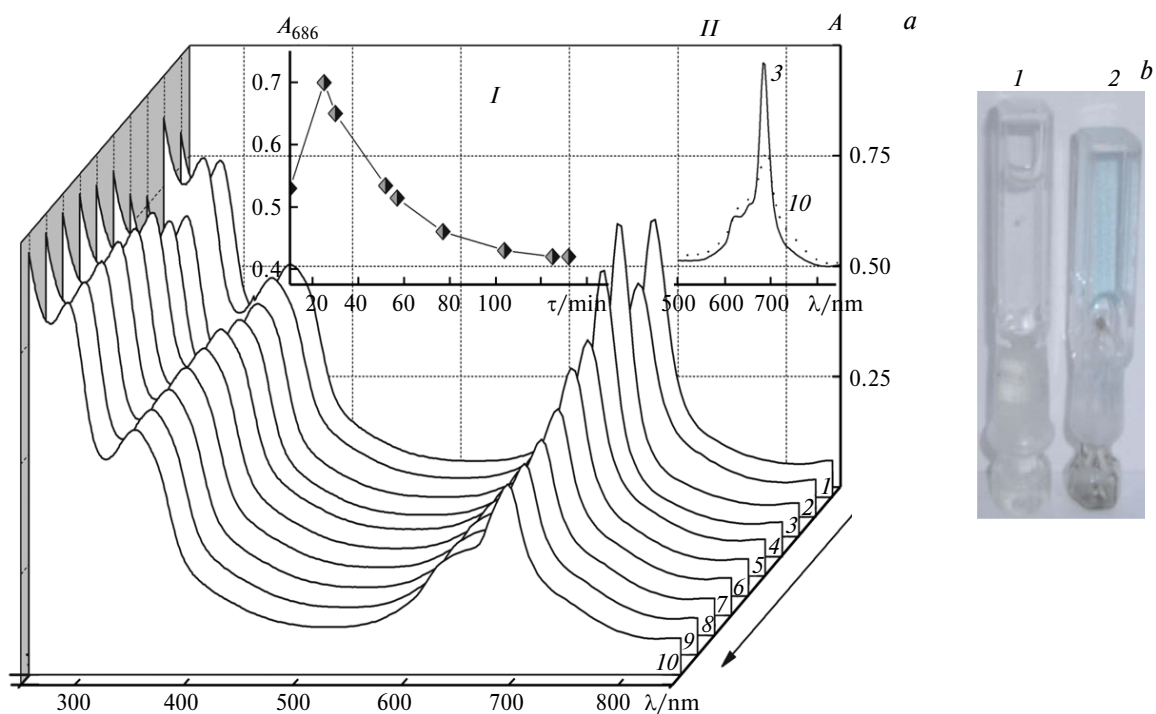


Fig. 15. (a) Changes in the EAS of direct gel (numbers 1–10 enumerate the spectra). Inset I: Formation of dense **1d**–SDC–Lys·HCl–NaCl–H₂O hydrogel from melt (55 °C) in the course of cooling the melt to room temperature (18 °C). Inset II: electronic absorption spectra of a solution (melt) of the hydrogel (spectrum 3) and dense **1d**–SDC–Lys·HCl–NaCl–H₂O hydrogel (spectrum 10). (b) Photographs of viscous fluid SDC–Lys·HCl (1) and **1d**–SDC–Lys·HCl hydrogel (2).⁶⁶

state which remains unchanged for a long period of time. The dense gel formed retains its shape and position in the vessel turned bottom up (conventional gel test) (Fig. 15, b) and exhibits the properties of a thixotropic liquid on vigorous shaking.

The formation of SDC gels involving electrostatic interactions, hydrogen bonds or their combination proceeds in aqueous solutions at nearly physiological pH values and requires a thorough choice of external parameters. Monovalent cations (in particular, cations of sodium deoxycholate or sodium chloride added to the system) play an important role in the formation and supramolecular organization of gels.^{38,64} Phthalocyanine-containing hydrogels are prepared by mixing components ("direct" gel) or by diffusion of Pc from aqueous solution to the gel formed from SDC and Lys·HCl ("diffuse" gel) at nearly physiological pH and ionic strength values.⁶⁵

Heating of the **1d**–SDC–Lys·HCl–NaCl hydrogel in the temperature range of 45–50 °C is accompanied by its melting (see Fig. 15, a, inset I). The temperature interval depends on the ratio of the components used to prepare the gel. As the phase state of the system changes, the EAS of the solubilized gel containing **1d** changes significantly, *viz.*, the optical density in the region of the Q-band increases and the Q-band shape changes (see Fig. 15, a, inset II). The absorption spectra of the system **1d**–SDC–Lys·HCl–NaCl–H₂O correspond to an increase in the concentration of monomeric **1d** upon change

in the phase state of the composite (melting). The state of phthalocyaninate **1d** in the molten hydrogel is similar to its state in the aqueous solution of the system **1d**–SDC–NaCl where the compound in question mainly exists in the monomeric form. Metallophthalocyanine-containing hydrogels exhibit a thermally reversible behavior, *viz.*, the heating–cooling cycle can be multiply repeated (Fig. 16, a).⁶⁶ The monomeric state of phthalocyaninate **1d** on melting of the gel was confirmed by fluorescence measurements, namely, the fluorescence intensity of thermally stimulated gel increased tenfold.⁶⁶

When dried in air, an SDC-containing supramolecular metallophthalocyanine-modified gel undergoes transition to a xerogel. The shape of the spectral lines in the EAS of gels and xerogels corresponds to the presence of a certain number of molecules of compound **1d** in the monomeric state; this is possible if the metallophthalocyanine molecule retains its local environment including SDC molecules or SDC–NaCl pairs upon drying. A fluorescence microscopy study revealed the appearance of bright spots that were interpreted as fluorescence of the phthalocyanine-containing supramolecular aggregates upon irradiation of samples at $\lambda = 633$ nm, which corresponds to excitation of phthalocyanine molecules; this was also confirmed by the EAS. Position of the Q-band maximum in the region characteristic of absorption of the monomeric state of the metallophthalocyanine is consistent with the fluorescence microscopy data that confirmed the presence of the mo-

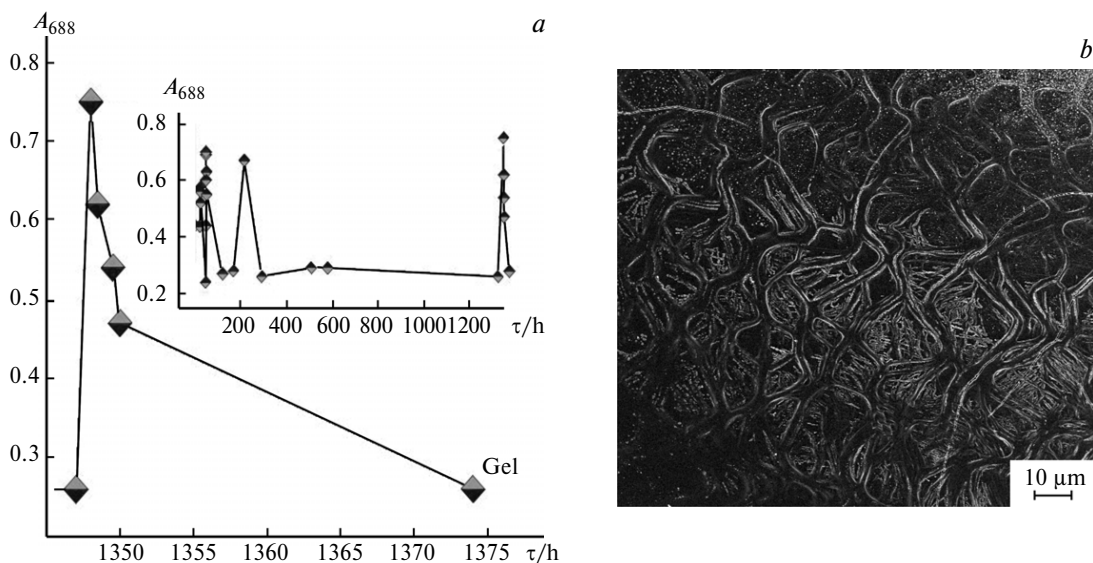


Fig. 16. Panel (a). Optical density of peak 3 (A_{688}) determined from deconvolution of the experimental absorption spectrum of the **1d**–SDC–Lys·HCl–NaCl–H₂O gel into Gaussian components plotted vs. time: gel (20 °C) → solution (~50 °C) → gel (20 °C). Shown is the repeating part of the graph. Inset: plot of A_{688} graph vs. time. Panel (b). SEM image of the **1d**–SDC–Lys·HCl–NaCl–H₂O aerogel.

meric form of compound **1d** in the xerogel,^{44,66} *viz.*, fluorescence of H-dimers and other Pc aggregates was quenched in accordance with the exciton theory.⁶⁷

Gels and xerogels containing compound **1d** were characterized by absorption and IR spectroscopies, X-ray diffraction, scanning electron microscopy (SEM), and fluorescence microscopy.⁶⁶ According to SEM data, the aerogel **1d**–SDC–Lys·HCl–NaCl–H₂O represents a 3D network structure composed of entangled fibers tens of micrometer long and to ten micrometer thick (Fig. 16, b). X-Ray diffraction experiments revealed no crystal structure in the SDC samples studied due to the formation of supramolecular phthalocyanine-containing gel based on SDC.

Metallophthalocyanines **1d**, **2b**, and **1e** in micellar solutions of SDC and STDC behave in a similar manner; however, no hydrogels formed in the presence of **1e** under identical conditions (concentrations of components, time). A hydrogel formed only upon adding SDC to the system, which is due to different hydrophobic/hydrophilic properties of these BS (see Table 3).

The addition of aqueous lysine hydrochloride solution to an aged **1d**–SDC–Lys·HCl–NaCl gel on melting or at room temperature leads to release of Pc. On going of compound **1d** from the gel to the aqueous phase the shape of the Q-band and position of its maximum were almost independent of the presence of lysine in the system (Fig. 17)

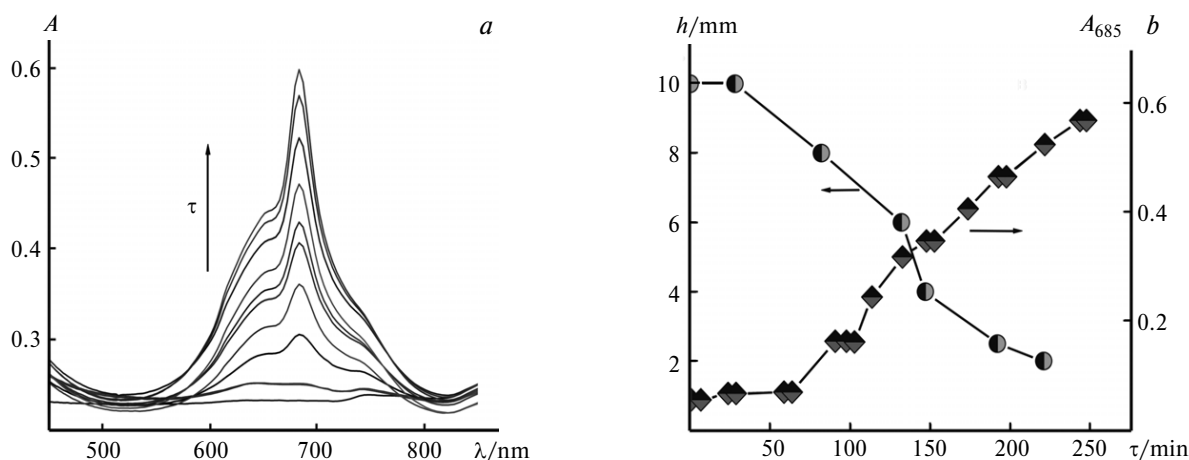


Fig. 17. Release of metallophthalocyanine **1d** from gel in the presence of lysine: changes in the optical density of the aqueous phase in the presence of lysine (a); a decrease in the gel layer thickness (h , mm) and an increase in the optical density (A_{685}) in the region of the Q-band in the aqueous layer (b).

compared to the spectrum of the micellar solution of **1d**—SDC—NaCl.⁶⁶

In physiological conditions ($[\text{NaCl}] = 0.137 \text{ mol L}^{-1}$, pH 7.4), a supramolecular gel containing SDC and the phosphoryl derivative of zinc phthalocyaninate **4** is formed. When dried at room temperature in air or in supercritical conditions, the gel is transformed to an aerogel that was characterized by the EAS and by fluorescence microscopy images.^{44,66}

Phthalocyanines as potential photosensitizers: supramolecular organization, cytotoxicity, and localization in tumor cells

Crown ethers interact with alkali and alkaline-earth metal ions to give guest—host complexes that simulate the functions of natural ionophores. Crown ether moieties at the periphery of the macrocycle enable dissolution of metallophthalocyanines in the aqueous medium and control their supramolecular organization in the microheterogeneous medium. These properties underlie the interest in phthalocyanines as potential photosensitizers.

The method of photodynamic therapy (PDT) is based on three nontoxic components, *viz.*, a photosensitizer, light, and oxygen. The photosensitizer is accumulated in tumor tissues. Irradiation of photosensitizer with light at a wavelength close to position of the absorption band maximum leads to generation of reactive oxygen species (ROS) including singlet oxygen ($^1\text{O}_2$) that have a cytotoxic effect on tumor cells.⁶⁸ Singlet oxygen is a strong oxidizer of saturated C—H bonds and unsaturated double bonds, as well as sulfide, amino, and other electron-donating groups in organic and biological molecules. The lifetime of $^1\text{O}_2$ in aqueous media is less than $2 \mu\text{s}$ ⁶⁹, being one or two orders of magnitude shorter than in other solvents.

Magnesium octa[(4'-benzo-15-crown-5)-oxy]phthalocyaninate **1d** was for the first time studied as a potential PDT agent. Eight crown ether substituents at the periphery of the macrocycle and the Mg^{2+} ion provide the solubility of **1d** in physiological conditions. Aqueous solutions of this compound as well as its solutions in the phosphate buffer demonstrate long-term stability in ambient conditions.

When in the PBS solution and in the DMEM* culture medium for HeLa cells, phthalocyaninate **1d** is in the aggregated state.⁷⁰ We assessed the cytotoxicity and photostability of compound **1d**, the photoinduced generation of ROS in the presence of **1d**, and studied the pattern of

its accumulation and localization in tumor cells. The light and dark toxicity IC_{50} (concentration of a compound, which reduces the MTT**-staining by 50%) is $1.83 \cdot 10^{-6} \text{ mol L}^{-1}$ and more than $25 \cdot 10^{-6} \text{ mol L}^{-1}$, respectively. Cell proliferation in the presence of metallophthalocyanine **1d** is inhibited in a dose-dependent manner. The morphology of HeLa cells remains almost unchanged at $[\mathbf{1d}] \leq 5 \cdot 10^{-6} \text{ mol L}^{-1}$. Changes observed with increasing $[\mathbf{1d}]$ probably originate from violation of the intracellular ion balance due to the presence of eight substituents bearing crown-5-ether groups at the periphery of the macrocycle.

The total concentration of ROS was determined using a DCFH₂ dye as detector; intracellular ROS cause oxidation of this compound to fluorescence-active 2',7'-dichlorofluorescein (DCF) characterized by an excitation maximum at 495 nm and an emission maximum at 529 nm⁷¹. The ROS concentrations expressed in units of DCF fluorescence intensity much exceed those in control set and reach a maximum value at $[\mathbf{1d}] = 12.5 \cdot 10^{-6} \text{ mol L}^{-1}$. At concentrations of **1d** close to its light toxicity (IC_{50} dose), the DCF fluorescence intensity rapidly increases. This is indicative of a high concentration of ROS generated upon laser irradiation of tumor cells in the presence of compound **1d** (670 nm, 30 min, 8 mW cm^{-2}) and thus of the photosensitizing effect of the phthalocyaninate.^{70,72}

The plot of the DCF fluorescence intensity (I_{fl}) vs. time reaches a plateau, which is probably due to the fact that almost no ROS are produced in the presence of compound **1d** accumulated in the HeLa cells in the chosen interval of observation times upon switching off of irradiation (Fig. 18). Fluorescence is emitted only by the DCF formed as a result of oxidation of the detector, DCFH₂, by the reactive species generated in the course of irradiation. These can be short-lived ROS incapable of initiating deeper oxidation stages (in particular, lipid peroxidation), *i.e.*, singlet oxygen.⁷³

The efficiency of PDT depends on the photophysical properties of the photosensitizer and on its accumulation and distribution in cells. Both fluorescence emission and intracellular ROS generation in the presence of phthalocyaninate **1d** indicate that the state of Pc accumulated in the cells differs significantly from its state in the DMEM culture medium (monomeric and aggregated state, respectively). A fluorescence microscopy image (Fig. 19) demonstrates that the signal from compound **1d** in the HeLa cells at $[\mathbf{1d}] = 5 \cdot 10^{-6} \text{ mol L}^{-1}$ and an incubation time of 24 h is uniform and that Pc mainly localizes in cytoplasm without toxic effect.⁷⁰ Crown ether groups favor transmembrane transfer of phthalocyaninate **1d**. A detailed

* Dulbecco's Modified Eagle Medium, or DMEM, is one of the most widely used artificial media for *in vitro* cultivation of mammal cells. Such media contain amino acids, vitamins, microelements, as well as additional supplementary components to ensure vitality and normal development of cells and tissues and support the necessary pH value.

** MTT is [3-(4,5-dimethylthiazol-2-yl)-2,5-diphenyl-2H-tetrazolium bromide], a yellow dye that is reduced to formazan, which has a purple color. The MTT assay is used to evaluate the number of viable cells present.

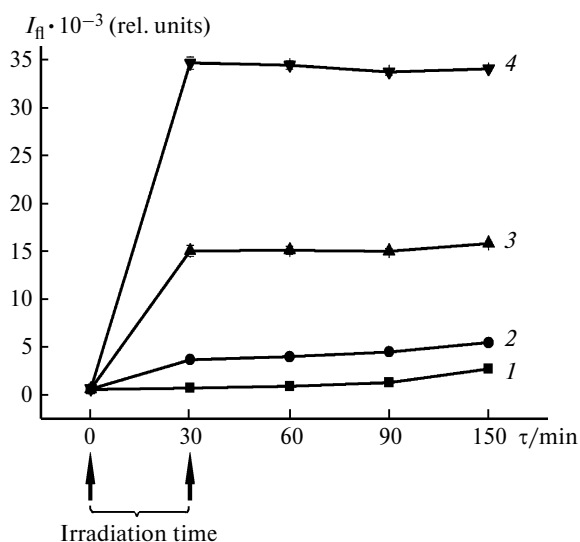


Fig. 18. Time dependence of fluorescence intensity (I_f) of DCF formed in the oxidation of DCFH₂ by photoinduced ROS in HeLa cells in the absence (1) and in the presence (2–4) of metallophthalocyanine **1d** upon cessation of irradiation.⁷² Concentration of compound **1d**: $1.56 \cdot 10^{-6}$ (2), $3.1 \cdot 10^{-6}$ (3), and $6.25 \cdot 10^{-6} \text{ mol L}^{-1}$ (4).

analysis of the samples using confocal microscopy showed that compound **1d** in the monomeric form localizes within cells in the perinuclear region and is not associated with nucleus components.⁷²

To gain a better insight into the intracellular action of photosensitizers, the kinetics were studied of oxidative photodynamic reactions proceeding on the surface of artificial membrane simulating a cell membrane. The method used involved measurements of the dipole potential on the membrane surface upon adsorption of a photosensitizer and subsequent irradiation. Experiments were carried out to study (i) the adsorption and photodynamic efficiency of sulfonated aluminum phthalocyaninate and *meso*-tetrakis(*p*-sulfonatophenyl)porphyrin on the surface of a bilayer lipid membrane and (ii) the behavior of singlet oxygen in the membrane, including deactivation of ¹O₂ by ceria nanoparticles.^{74–77} Solutions of aluminum(III), gallium(III), and indium(III) hydroxide tetra-15-crown-5-phthalocyaninates were used as photosensitizers.

Substitution at non-peripheral α -positions of the macrocycle causes a bathochromic shift of the Q-band maximum in the absorption spectrum of the monomer, an increase in the solubility of Pc, and can, in principle, lead to reduction of the aggregative ability of the compound. As an example, the spectral, photophysical and photochemical properties of α -octa-butoxy-substituted phthalocyanine and its metal complexes ($M = \text{Mg}^{2+}, \text{Zn}^{2+}, \text{Ga}^{3+}, \text{In}^{3+}$) in DMSO solutions were studied.⁷⁸ Based on the absorption spectra, these compounds exist in the monomeric state while their Q-band maxima and fluorescence emission peaks are in the range of 746–780 and 768–813 nm, respectively. The quantum yield of fluorescence of the compounds in question was at most 5% while

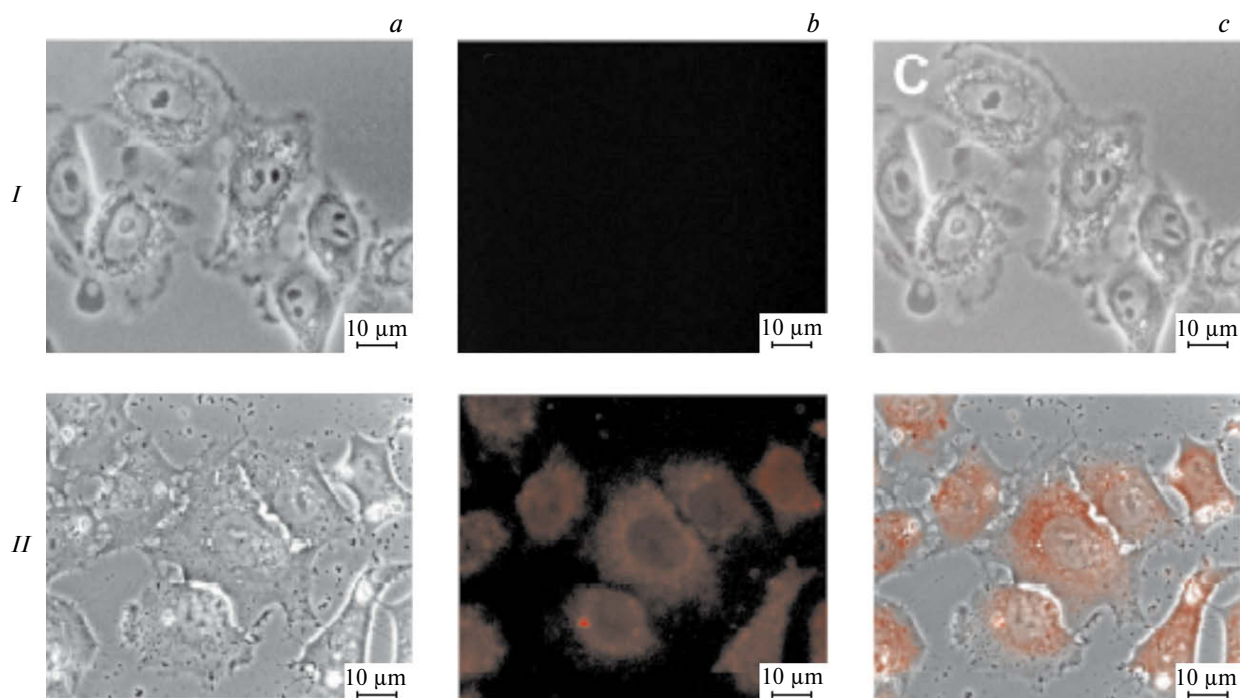


Fig. 19. Localization of phthalocyaninate **1d** in HeLa cells (without fixation). Lines: I (a–c) — unprocessed cells, II (a–c) — cells processed with $[\mathbf{1d}] = 5 \cdot 10^{-6} \text{ mol L}^{-1}$ for 24 h. Columns: a (I,II) — phase contrast, b (I,II) — accumulation/localization of **1d** in the cells; and c (I,II) — merging (scale bar 10 μm)⁷⁰.

that of $^1\text{O}_2$ varied from 4% (PcH_2) to 36% (PcZn). The photostability of these Pc under laser irradiation ($\lambda = 670 \text{ nm}$) decreased in the order $\text{PcGaCl} > \text{PcInCl} > \text{PcZn} > \text{PcMg} > \text{PcH}_2$. Simulation of the generation of ROS including singlet oxygen and their transport through an artificial membrane is of interest from the standpoint of research into processes occurring in living cells upon excitation in the presence of a sensitizer and can undoubtedly be useful for further studies of various systems including those discussed in this review.

Conclusion

Investigation of supramolecular assembly of systems in aqueous media is a dynamically developing field of scientific research. This knowledge is important for better understanding and control of the key processes proceeding in wildlife and for solving certain problems in medicine and biology. In this connection the development of methods for solubilization of hydrophobic coordination compounds that are thought to possess biological activity is a topical problem in modern chemistry. Taking crown- and phosphoryl-substituted phthalocyanines and their metal complexes as examples, in this review we demonstrated the possibility to solve this problem using the supramolecular approach. We have shown that optimum conditions for solubilization and deaggregation of phthalocyanines in aqueous media through formation of supramolecular assemblies can be established by properly combining surfactants of different nature and the ability of crown ethers to form guest–host complexes that simulate functions of natural ionophores.

Solubilization of phthalocyanines involves various types of noncovalent interactions. Namely, the formation of phthalocyanine-containing supramolecular assemblies is possible in the case of synergistic effect of (i) complexation of K^+ or Na^+ ions with the crown ether fragments of Pc, (ii) electrostatic interaction between the polar group ($-\text{OSO}_3^-$, for SDS) and the complex-bound Na^+ ion, and (iii) hydrophobic interactions. Solubilization of Pc in the microheterogeneous aqueous media based on BS is influenced by the number of crown ether substituents and by the method for introducing them into the macrocycle. The effect of the structure and size of the surfactant cation on dissolution of crown-containing Pc in aqueous media was studied. It was shown that phosphoryl-containing zinc phthalocyaninate **4** exists in solution in the presence of CTPB in the micelle-bound monomeric state similarly to solutions of CTAB.⁴⁴ Solubilization of octa-crown-substituted magnesium phthalocyaninate **1d** in the presence of CTPB implies incorporation of the crown ether groups of Pc into cavities between phenyl rings of cetyltriphenylphosphonium cation⁷⁹ due to possible short contacts $\text{O}\cdots\text{H}$ or $\text{C}\cdots\text{H}$ since the hydrodynamic radius of this

cation (2.1 nm)⁸⁰ is noticeably larger than the diameter of the crown-5-ether cavity (1.7–2.2 Å). Amphiphilic phosphonium salts are cationic surfactants with higher aggregative and solubilizing ability, while lipophilic phosphonium cations are able to cross the mitochondrial membranes without the assistance of ionophores.^{80,81} Taking account of low cmc of salts, this is of great importance for PDT, since cell mitochondria represent oxygen "banks".

Monomerization of annelated tetra-15-crown-5-substituted magnesium phthalocyaninate **3** in BS is very attractive. Bile salts are considered as potential systems for drug delivery to biological targets, which facilitate passage through the hydrophobic barrier. For instance, an analysis of the intensity ratio of the first and third vibronic peaks (I_1/I_3) in the fluorescence emission spectrum of pyrene in water and in micellar solutions of BS (see Table 3) showed that pyrene molecules in SC, SDC, STC, and STDC are in the nonpolar (hydrocarbon) environment.³⁹ Fluorescence of phthalocyaninates **1d** and **4** in the microheterogeneous medium of BS or SDS confirms their monomeric state in the supramolecular assemblies and points to shielding of the Pc molecules (like pyrene) from the aqueous medium. Monomeric state of compound **4** in the microheterogeneous media based on anionic surfactants (BS and SDS) is probably due to the presence of pentyl group in the phosphoryl moiety and its solubilization in the hydrophobic cavities or in the nearest environment of micelles.

Owing to differences between conventional surfactants and BS, self-assembly of amphiphilic BS molecules in aqueous media leads to formation of various supramolecular structures from small (micelles) to large (nanofibers, nanotubes, and nanoribbons), and then to supramolecular hydrogels based on these structures. For the first time, crown-substituted magnesium and zinc phthalocyaninates were solubilized in aqueous medium in the presence of SDC and supramolecular hydrogels containing Pc as active component were prepared within the framework of the supramolecular approach. Amino acids *in vitro* weaken gels and favor the release of phthalocyanine.

We believe that information on supramolecular organization of crown- and phosphoryl-substituted Pc in aqueous microheterogeneous media, photobiological properties of compound **1d** in HeLa cells, and monomeric state of phthalocyaninate **4** in solutions of biocompatible amphiphilic polymers is of interest for PDT applications. The results obtained allows one to continue investigations of this type of phthalocyanines and their metal complexes as photosensitizers from the standpoint of reducing the general toxicity of crown-substituted Pc, specification of cell organelles with accumulated Pc, as well as photochemical and photobiological properties of type-**4** compounds in solutions of biocompatible polymers.

The review was prepared under financial support from the Ministry of Science and Education of the Russian

Federation (under Contract Nos AAAA-A19-11907189 0015-6 and 0120.0504026), the Russian Academy of Sciences (as part of Program 14.P), and under partial financial support from the Russian Foundation for Basic Research (Project No. 18-03-00743) and the Council on Grants at the President of the Russian Federation (State Support of Leading Scientific Schools, Grant No. NSh-3867.2018.3).

References

1. J.-M. Lehn, *Pure Appl. Chem.*, 1978, **50**, 871; DOI: 10.1351/pac197850090871.
2. M. Nishio, *Tetrahedron*, 2005, **61**, 6923; DOI: 10.1016/j.tet.2005.04.041.
3. N. F. Goldshleger, A. F. Shestakov, E. V. Ovsyannikova, N. M. Alpatova, *Russ. Chem. Rev.*, 2008, **77**, 815; DOI: 10.1070/RC2008v077n09ABEH003877.
4. A. F. Shestakov, D. V. Konarev, S. V. Simonov, S. S. Khasanov, A. N. Lapshin, N. F. Goldshleger, *RSC Adv.*, 2013, **3**, 8341; DOI: 10.1039/C3RA22787A.
5. G. P. Shaposhnikov, V. P. Kulinich, V. E. Mayzlish, *Modifitsirovannyye ftalotsyaniny i ikh strukturnyye analogi [Modified Phthalocyanines and Their Structural Analogues]*, Ed. O. I. Koifman, 2nd Ed., Moscow, KRASAND, Ivanovo State Chem. Technol. Univ., 2012, 480 pp. (in Russian).
6. I. P. Beletskaya, V. S. Tyurin, A. Yu. Tsivadze, R. Gillard, C. Stern, *Chem. Rev.*, 2009, **109**, 1659; DOI: 10.1021/cr800247a.
7. A. Y. Tsivadze, L. A. Nosikova, Z. A. Kudryashova, *Protect. Metals Phys. Chem. Surfaces (Engl. Transl.)*, 2012, **48**, 135; DOI: 10.1134/S2070205112020190.
8. E. A. Lukyanets, *J. Porphy. Phthal.*, 1999, **3**, 424; DOI: 10.1002/(SICI)1099-1409(199908/10)3:6/7<424::AID-JPP151>3.3.CO;2-B.
9. E. A. Lukyanets, *Photodyn. Therapy and Photodiagnosics*, 2013, **2**, No. 3, 3 (in Russian).
10. R. I. Yakubovskaya, N. B. Morozova, A. A. Pankratov, N. I. Kazachkina, A. D. Plyutinskaya, T. A. Karmakova, T. N. Andreeva, Yu. B. Venediktova, E. A. Plotnikova, E. R. Nemtsova, V. V. Sokolov, E. V. Filonenko, V. I. Chissov, B. Ya. Kogan, A. V. Butenin, A. V. Feofanov, M. G. Strakhovskaya, *Russ. J. Gen. Chem.*, 2015, **85**, 217; DOI: 10.1134/S1070363215010405.
11. A. Yu. Tsivadze, *Russ. Chem. Rev.*, 2004, **73**, 5; DOI: 10.1070/RC2004v073n01ABEH000862.
12. Yu. G. Gorbunova, A. G. Martynov, A. Yu. Tsivadze, in *Handbook of Porphyrin Science: Coordination Chemistry and Materials*, Vol. 24, Eds K. M. Kadish, K. M. Smith, R. Guilard, World Scientific Publishing, New Jersey—London—Singapore—Beijing—Shanghai—Hong Kong—Taipei—Chennai, 2012, p. 271.
13. N. M. Logacheva, V. E. Baulin, A. Y. Tsivadze, T. V. Basova, L. A. Sheludyakova, *Russ. Chem. Bull.*, 2008, **57**, 1467; DOI: 10.1007/s11172-008-0190-9.
14. C. J. Pedersen, *J. Am. Chem. Soc.*, 1967, **89**, 2495.
15. E. V. Ovsyannikova, N. F. Goldshleger, N. M. Kurochkina, V. E. Baulin, A. Yu. Tsivadze, N. M. Alpatova, *Makrogeterotsikly [Macroheterocycles]*, 2010, **3**, 125 (in Russian); DOI: 10.6060/mhc2010.2-3.125.
16. Y. Marcus, *Ion Solvation*, Wiley and Sons, Chichester—New York—Brisbane—Toronto—Singapore, 1985, 306 p.
17. C. J. Huang, I. Favre, E. Moczydlowski, *J. Gen. Physiol.*, 2000, **115**, 43.
18. K. Seyrek, G. Gecher, *Polymer Sci., A*, 2012, **7**, 159.
19. V. E. Baulin, E. V. Ovsyannikova, I. P. Kalashnikova, G. P. Girina, V. N. Andreev, N. M. Alpatova, A. Yu. Tsivadze, *Protect. Metals Phys. Chem. Surfaces (Engl. Transl.)*, 2013, **49**, 5; DOI: 10.1134/S2070205113010048.
20. K. Holmberg, B. Jönsson, B. Kronberg, B. Lindman, *Surfactants and Polymers in Aqueous Solution*, 2nd Ed., 2003, Wiley, Chichester.
21. D. Yu, F. Huang, H. Xu, *Analytical Methods*, 2012, **4**, 47; DOI: 10.1039/C1AY05495C.
22. X.-Y. Lu, Y. Jiang, X.-H. Cui, S.-Z. Mao, M.-L. Liu, Y.-R. Du, *Acta Phys.-Chim. Sin.*, 2009, **25**, 1357; DOI: 10.3866/PKU.WHXB20090714.
23. S. Kumar, D. Sharma, D. Sharma, Kabir-ud-Din, *J. Surf. Deterg.*, 2006, **9**, 77; DOI: 10.1007/s11743-006-0378-7.
24. A. Chatterjee, S. P. Moulik, S. K. Sanyal, B. K. Mishra, P. M. Puri, *J. Phys. Chem. B*, 2001, **105**, 12823; DOI: 10.1021/jp0123029.
25. E. Y. Sheu, S.-H. Chen, J. S. Huang, *J. Phys. Chem.*, 1987, **91**, 3306.
26. R. Ninomiya, K. Matsuoka, Y. Moroi, *Biochim. Biophys. Acta*, 2003, **1634**, 116; DOI: 10.1016/j.bbali.2003.09.003.
27. N. F. Goldshleger, I. P. Kalashnikova, V. E. Baulin, A. Yu. Tsivadze, *Protect. Metals Phys. Chem. Surfaces (Engl. Transl.)*, 2011, **47**, 471; DOI: 10.1134/S2070205111040071.
28. X. O. Wang, L. Li, H. Ye, K. Yang, Y. P. Wang, D. J. Sandman, *J. Macromol. Sci., Pure Appl. Chem.*, 2007, **44**, 1323; DOI: 10.1080/10601320701610754.
29. N. Kobayashi, M. Togashi, T. Osa, K. Ishii, S. Yamauchi, H. Hino, *J. Am. Chem. Soc.*, 1996, **118**, 1073.
30. N. F. Goldshleger, V. E. Baulin, A. Yu. Tsivadze, *Protect. Metals Phys. Chem. Surfaces (Engl. Transl.)*, 2014, **50**, 135; DOI: 10.1134/S2070205114020087.
31. N. F. Goldshleger, A. V. Chernyak, I. P. Kalashnikova, V. E. Baulin, A. Yu. Tsivadze, *Russ. J. Gen. Chem.*, 2012, **82**, 927; DOI: 10.1134/S1070363212050210.
32. N. F. Goldshleger, A. V. Chernyak, A. S. Lobach, I. P. Kalashnikova, V. E. Baulin, A. Y. Tsivadze, *Protect. Metals Phys. Chem. Surfaces (Engl. Transl.)*, 2015, **51**, 212; DOI: 10.1134/S2070205115020070.
33. S. A. Tovstun, V. F. Razumov, *Russ. Chem. Rev.*, 2011, **80**, 953.
34. N. F. Goldshleger, V. Yu. Gak, I. P. Kalashnikova, V. E. Baulin, A. V. Ivanchikhina, V. A. Smirnov, A. A. Shiryaev, A. Yu. Tsivadze, *Protect. Metals Phys. Chem. Surfaces (Engl. Transl.)*, 2018, **54**, 1092; DOI: 10.1134/S2070205118060126.
35. K. P. Birin, Yu. G. Gorbunova, A. Yu. Tsivadze, *Protect. Metals Phys. Chem. Surfaces (Engl. Transl.)*, 2011, **47**, 417; DOI: 10.1134/S2070205111040058.
36. M. Miyata, K. Sada, Y. Miyake, in *Organized Assemblies in Chemical Analysis*, Vol. 2, Ed. W. L. Hinze, 2000, JAI Press, Stamford, p. 205.
37. H. Svobodova, V. Noponen, E. Kolehmainen, E. Sievanen, *RSC Adv.*, 2012, **2**, 4985; DOI: 10.1039/C2RA01343F.

38. N. F. Goldshleger, A. S. Lobach, V. E. Baulin, A. Yu. Tsivadze, *Russ. Chem. Rev.*, 2017, **86**, 269; DOI: 10.1070/RCR4682.
39. B. Mukherjee, A. A. Dar, P. A. Bhat, S. P. Moulik, A. R. Das, *RSC Adv.*, 2016, **6**, 1769; DOI: 10.1039/C5RA20909A.
40. M. H. Najjar, O. A. Chat, A. A. Dar, G. M. Rather, *J. Surfact. Deterg.*, 2013, **16**, 967; DOI: 10.1007/s11743-013-1443-7.
41. S. Das, J. Dey, T. Mukhim, K. Ismail, *J. Colloid Interface Sci.*, 2011, **357**, 434; DOI: 10.1016/j.jcis.2011.02.020.
42. J. Janczak, *Polyhedron*, 2010, **29**, 941; DOI: 10.1016/j.poly.2009.11.001.
43. N. F. Goldshleger, A. S. Lobach, V. Yu. Gak, I. P. Kalashnikova, V. E. Baulin, A. Yu. Tsivadze, *Protect. Metals Phys. Chem. Surfaces (Engl. Transl.)*, 2014, **50**, 599; DOI: 10.1134/S2070205114050086.
44. N. F. Goldshleger, V. Y. Gak, M. A. Lapshina, V. E. Baulin, A. A. Shiryaev, A. Y. Tsivadze, *Russ. Chem. Bull.*, 2018, **67**, 2205; DOI: 10.1007/s11172-018-2357-3.
45. Y. Shiraiishi, S. Sumiya, Y. Kohno, T. Hirai, *J. Org. Chem.*, 2008, **73**, 8571; DOI: 10.1021/jo8012447.
46. L. B. Pártay, P. Jedlovsky, M. Segá, *J. Phys. Chem. B*, 2007, **111**, 9896; DOI: 10.1021/jp072974k.
47. V. E. Baulin, G. S. Tsebrikova, D. V. Baulin, Y. F. Al Ansary, *Biomed. Chem.: Res. Methods*, 2018, **1**, No. 3, e00043; DOI: 10.18097/BMCRM00043.
48. S. K. Verma, K. K. Ghosh, *J. Surfact. Deterg.*, 2011, **14**, 347; DOI: 10.1007/s11743-010-1237-0.
49. L. A. Lapkina, Yu. G. Gorbunova, D. O. Gil, V. K. Ivanov, N. Yu. Konstantinov, A. Yu. Tsivadze, *J. Porph. Phthal.*, 2013, **17**, 564; DOI: 10.1142/S1088424613500648.
50. L. A. Lapkina, V. E. Larchenko, G. A. Kirakosyan, A. Yu. Tsivadze, S. I. Troyanov, Yu. G. Gorbunova, *Inorg. Chem.*, 2018, **57**, 82; DOI: 10.1021/acs.inorgchem.7b01983.
51. N. F. Goldshleger, I. P. Kalashnikova, Y. G. Gorbunova, A. G. Martynov, V. E. Baulin, A. Yu. Tsivadze, *Protect. Metals Phys. Chem. Surfaces (Engl. Transl.)*, 2018, **54**, 33; DOI: 10.1134/2070205118010082.
52. E. A. Safonova, A. G. Martynov, S. E. Nefedov, G. A. Kirakosyan, Yu. G. Gorbunova, A. Yu. Tsivadze, *Inorg. Chem.*, 2016, **55**, 2450; DOI: 10.1021/acs.inorgchem.5b02831.
53. D. R. Anderson, P. V. Solntsev, H. M. Rhoda, V. N. Nemykin, *J. Porph. Phthal.*, 2016, **20**, 337; DOI: 10.1142/S1088424616500164.
54. R. Li, E. Carpentier, E. D. Newell, L. M. Olague, E. Heafey, C. Yihwa, C. Bohne, *Langmuir*, 2009, **25**, 13800; DOI: 10.1021/la901826y.
55. N. F. Goldshleger, A. B. Kornev, A. V. Barinov, P. A. Troshin, A. I. Kotel'nikov, V. E. Baulin, A. Yu. Tsivadze, *Russ. Chem. Bull.*, 2012, **61**, 1242; DOI: 10.1007/s11172-012-0168-5.
56. N. F. Goldshleger, V. Yu. Gak, A. S. Lobach, I. P. Kalashnikova, V. E. Baulin, A. Yu. Tsivadze, *Makroeterotsikly [Macroheterocycles]*, 2015, **8**, 343; DOI: 10.6060/mhc151083g].
57. E. V. Ovsyannikova, A. A. Shiryaev, I. P. Kalashnikova, V. E. Baulin, A. Yu. Tsivadze, V. N. Andreev, N. M. Alpatova, *Makroeterotsikly [Macroheterocycles]*, 2013, **6**, 274 (in Russian); DOI: 10.6060/mhc130745a].
58. J. Santhanalakshmi, G. Santhanalakshmi, V. K. Aswal, P. S. Goyal, *Proc. Ind. Acad. Sci. (Chem. Sci.)*, 2001, **113**, 55; <https://www.ias.ac.in/article/fulltext/jcsc/113/01/0055-0062>.
59. G. Yu, X. Yan, C. Han, F. Huang, *Chem. Soc. Rev.*, 2013, **42**, 6697; DOI: 10.1039/C3CS60080G.
60. L. E. Buerkle, S. J. Rowan, *Chem. Soc. Rev.*, 2012, **41**, 6089; DOI: 10.1039/C2CS35106D.
61. S. S. Babu, V. K. Praveen, A. Ajayaghosh, *Chem. Rev.*, 2014, **114**, 1973; DOI: 10.1021/cr400195e.
62. S. Mukhopadhyay, U. Maitra, *Curr. Sci.*, 2004, **87**, 1666.
63. Y. Zhang, X. Xin, J. Shen, W. Tang, Y. Ren, L. Wang, *RSC Adv.*, 2014, **4**, 62262; DOI: 10.1039/C4RA13353F.
64. H. Wang, W. Xu, S. Song, L. Feng, A. Song, J. Hao, *J. Phys. Chem. B.*, 2014, **118**, 4693; DOI: 10.1021/jp500113h.
65. N. F. Goldshleger, V. Y. Gak, A. S. Lobach, I. P. Kalashnikova, V. E. Baulin, A. Y. Tsivadze, *Protect. Metals Phys. Chem. Surfaces (Engl. Transl.)*, 2018, **54**, 174; DOI: 10.1134/S2070205118020053.
66. N. F. Goldshleger, A. S. Lobach, N. N. Dremova, M. A. Lapshina, A. M. Kolesnikova, V. E. Baulin, A. Yu. Tsivadze, *Makroeterotsikly [Macroheterocycles]*, 2017, **10**, 531; DOI: 10.6060/mhc170830g.
67. M. Kasha, H. R. Rawis, M. A. El-Bayoumi, *Pure Appl. Chem.*, 1965, **11**, 371; DOI: 10.1351/pac196511030371.
68. S. Wang, R. Gao, F. Zhou, M. Selke, *J. Mater. Chem.*, 2004, **14**, 487; DOI: 10.1039/B311429E.
69. *Einführung in die Photochemie*, Ed. H. O. Becker, Wiley-VCH Verlag, Weinheim, 1976, 486 p.
70. M. A. Lapshina, S. I. Norko, V. E. Baulin, A. A. Terentiev, A. Yu. Tsivadze, N. F. Goldshleger, *Makroeterotsikly [Macroheterocycles]*, 2018, **11**, 396; DOI: 10.6060/mhc180899l.
71. X. Chen, Z. Zhong, Z. Xu, L. Chen, Y. Wang, *Free Radical Res.*, 2010, **44**, 587; DOI: 10.3109/10715761003709802.
72. M. A. Lapshina, V. E. Baulin, A. A. Ustyugov, A. A. Terentyev, N. F. Goldshleger, *Abstracts of 4th Russ. Conf. on Medicinal Chemistry with international participants "MedChem Russia 2019" (Ekaterinburg, June 9–14, 2019)*, Ural Branch of the Russian Academy of Sciences, 2019, p. 369.
73. N. A. Daghasanli, R. Itri, M. S. Baptista, *Photochem. Photobiol.*, 2008, **84**, No. 5, 1238; DOI: 10.1111/j.1751-1097.2008.00345.x.
74. V. S. Sokolov, A. N. Gavrilchik, A. O. Kulagina, I. N. Meshkov, P. Pohl, Yu. G. Gorbunova, *J. Photochem. Photobiol. B: Biology*, 2016, **161**, 162; DOI: 10.1016/j.jphotobiol.2016.05.016.
75. A. N. Konstantinova, V. S. Sokolov, I. Jiménez-Munguía, O. A. Finogenova, Yu. A. Ermakov, Yu. G. Gorbunova, *J. Photochem. Photobiol. B: Biology*, 2018, **189**, 74; DOI: 10.1016/j.jphotobiol.2018.10.001.
76. T. O. Shekunova, L. A. Lapkina, A. B. Shcherbakov, I. N. Meshkov, V. K. Ivanov, A. Yu. Tsivadze, Yu. G. Gorbunova, *J. Photochem. Photobiol. A: Chem.*, 2019, **382**, 111925; DOI: 10.1016/j.jphotochem.2019.111925.
77. V. S. Sokolov, O. V. Batishchev, S. A. Akimov, T. R. Galimzyanov, A. N. Konstantinova, E. Malingrioux, Y. G. Gorbunova, D. G. Knyazev, P. Pohl, *Sci. Rep.*, 2018, **8**, Art.N 14000; DOI: 10.1038/s41598-018-31901-9.
78. E. A. Safonova, I. N. Meshkov, M. V. Polovkova, A. Yu. Tsivadze, Yu. G. Gorbunova, *Mendelev Commun.*, 2018, **28**, 275; DOI: 10.1016/j.mencom.2018.05.015.
79. T. G. Movchan, A. A. Averin, D. V. Baulin, E. V. Plotnikova, V. E. Baulin, A. Y. Tsivadze, *Colloid. J. (Engl. Transl.)*, 2018, **80**, 501; DOI: 10.1134/S1061933X18050095 [*Kolloid Zh.*, 2018, **80**, 528].

80. G. I. Vagapova, F. G. Valeeva, G. A. Gainanova, V. V. Syakaev, I. V. Galkina, L. Ya. Zakharova, S. K. Latypov, A. I. Konovalov, *Colloids Surf., A*, 2013, **419**, 186; DOI: 10.1016/j.colsurfa.2012.11.071. 2005, **70**, 222; DOI: 10.1007/s10541-005-0104-5 [*Biokhimiya*, 2005, **70**, 273].
81. M. F. Ross, G. F. Kelso, F. H. Blaikie, A. M. James, H. M. Cochemé, A. Filipovska, T. Da Ros, T. R. Hurd, R. A. J. Smith, M. P. Murphy, *Biochemistry (Moscow) (Engl. Transl.)*, *Received September 30, 2019;*
in revised form November 18, 2019;
accepted April 30, 2020
-